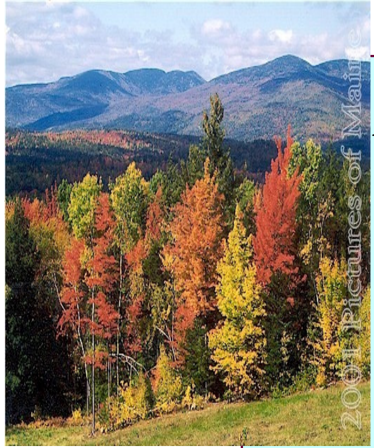

A Coupled Leaf/Canopy Turbid Medium Radiative Transfer Model

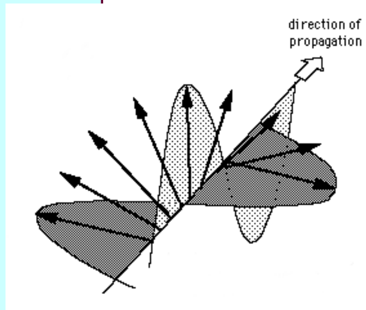

Barry D. Ganapol
Departments of Hydrology and Water Resources
and
Aerospace and Mechanical Engineering

University of Arizona
520/621-4728
ganapol@cowboy.ame.arizona.edu

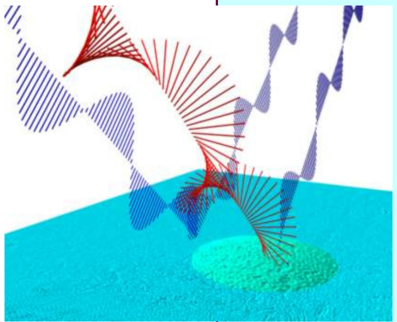

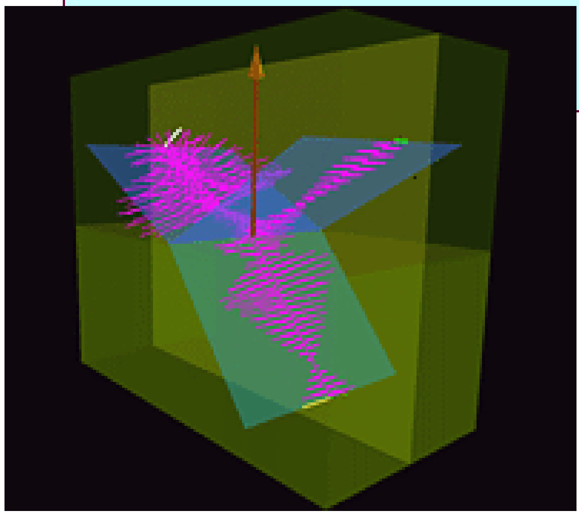

Fundamental science issue?

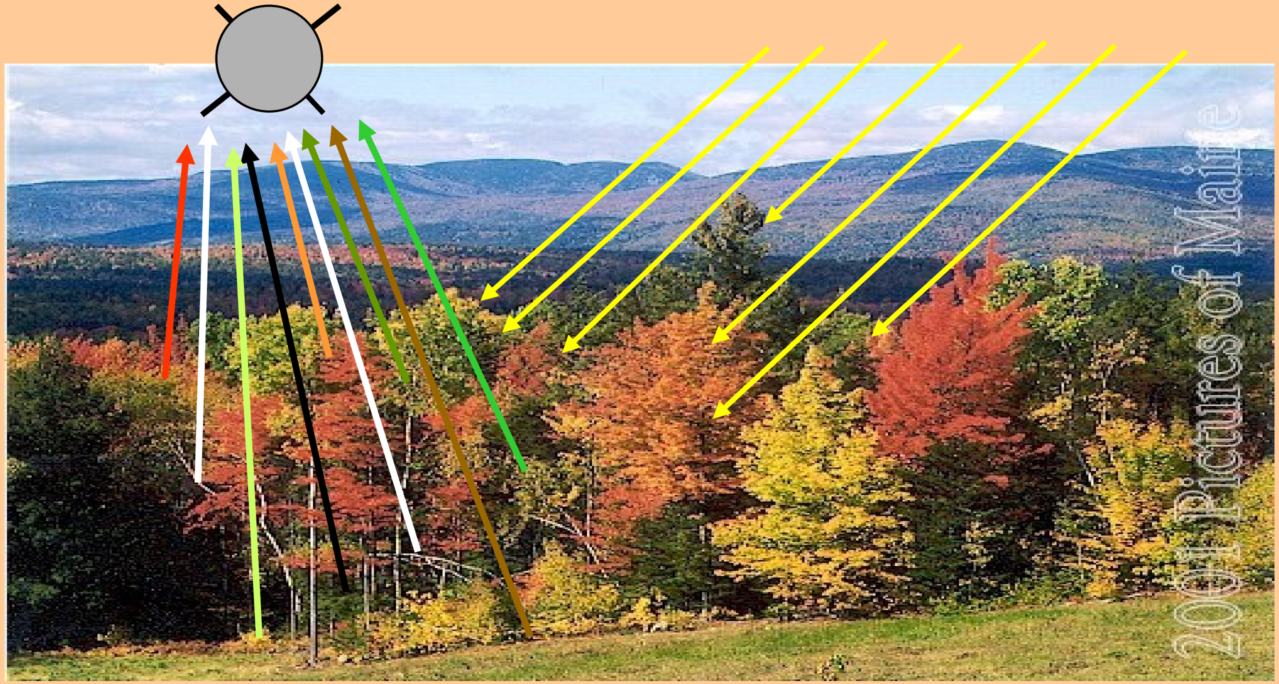

Light is transmitted through the atmosphere and reflected from vegetation canopy elements and background to an air or space borne sensor.

Can the reflected information be ^reliably interpreted through the vegetation canopy reflectance?

What social implications will the reliable interpretation of reflected information from foliage have?

- Basic Science
  - + Photosynthesis
  - + Establish ecological principles
- Precision Agriculture
  - + Improved crop yield
  - + Improved crop management
- Global climate change prediction
  - + Terrestrial surface reflectance
  - + **GCM** verification and validation
- **P**recision **B**attlefield **E**ngagement (**PBE**)
  - + Warfighter asset management
  - + Adversary asset strength and location

General CR Modeling Considerations

■ **Vegetation signatures**:

+ Spectral λ: Wavelength response of canopy element (R_f, T_n, A_b)
+ Spatial (x,y): arrangement of scattering objects within canopy
+ Temporal (t): intra- and inter- annual variability
+ Directional (Ω): anisotropy resulting from surface roughness
+ Polarization: (Q): polarized state of surface reflected photons

■ **Factors influencing reflectance:**

+ size, shape and distribution of canopy phytoelements
+ biophysical parameters: Leaf Area Index (LAI)
fAPAR
leaf optical properties
Leaf Angle Distribution (LAD)

Presentation:

- Focus on turbid medium model **LCM2**
  - Describe the microscopic leaf radiative transfer model
  - Describe the macroscopic leaf radiative transfer model in the canopy
  - **LCM2 P**olarization (**LCM2P**) algorithm
- Demonstrate application of **LCM2**

General Turbid Medium Canopy Modeling Considerations

Elements of a canopy reflectance model

+ Phytoelements

  <u>Broadleaves</u>

  Needleleaves

+ Leaf canopy

Radiative Transfer (**RT**) considerations:

+ Intra-leaf
+ Inter-leaf

} scattering and absorption

Complicated participating medium

+ Not a well posed **RT** problem
+ Ignorant of biophysical properties and configurations
+ Must rely on natural averaging
  and a little luck

Leaf Scattering

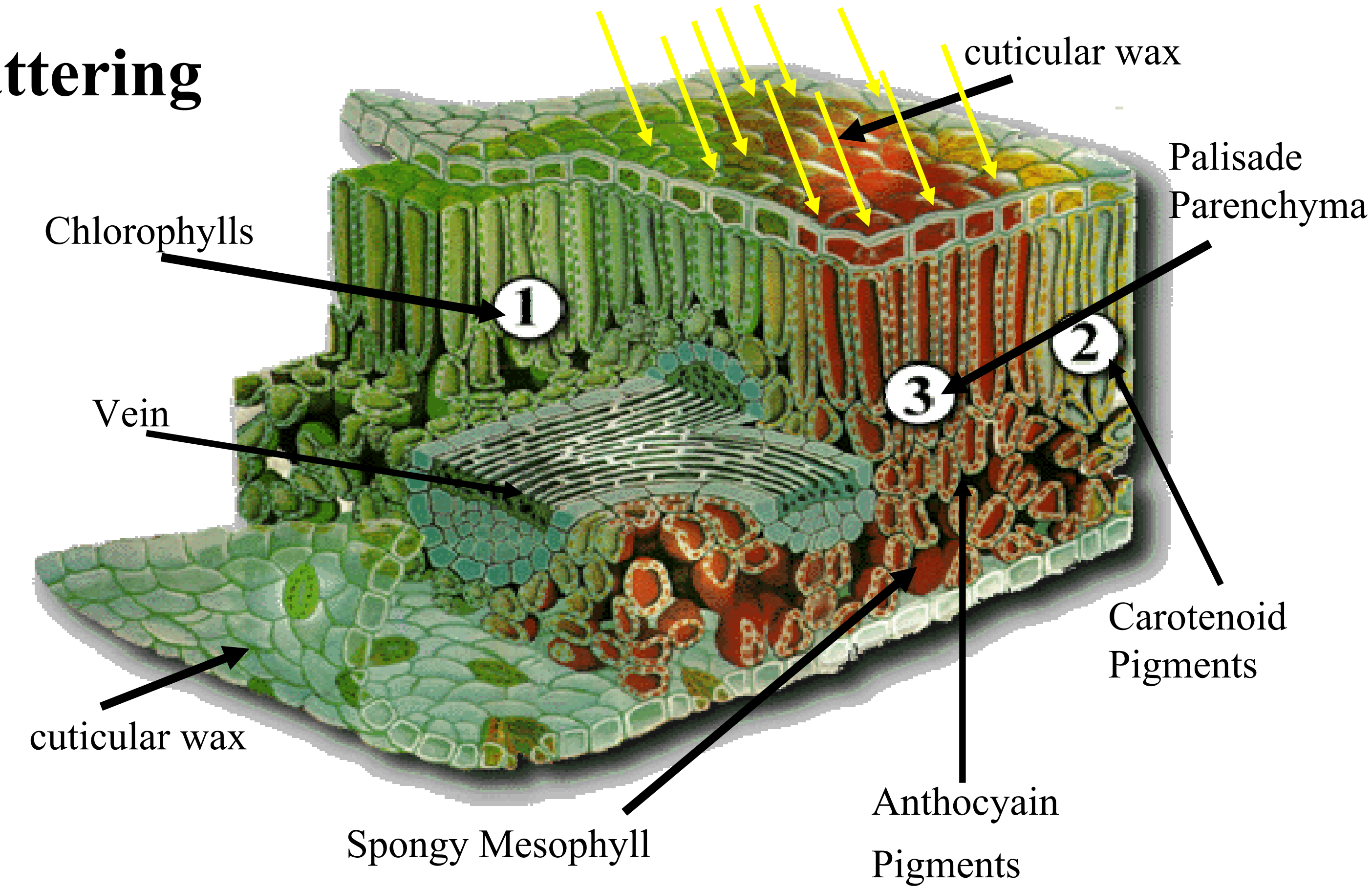

Typical anatomical structure of a leaf

+ Air-epicuticular wax interface (upper epidermis)
  - thin wax film
  - multilayered membrane of pectin, cellulose, cutin and wax
+ Palisade Parenchyma
+ Spongy Mesophyll
+ Epicuticular wax -air interface (lower epidermis)

■ Leaf Scattering Phase Function (Microscopic)

+ Microscopic leaf radiative transfer

$$\left[\Omega\frac{\partial}{\partial\tau}+1\right]I\left(\tau,\Omega;\Omega_0\right)=\frac{\omega}{4\pi}\int_{4\pi} d\Omega' I\left(\tau,\Omega';\Omega_0\right)$$

$$I\left(0,\Omega;\Omega_0\right)=\delta\left(\Omega-\Omega_0\right)$$

$$I\left(\Delta_L,\Omega\left(-\mu,\phi\right);\Omega_0\right)=0$$

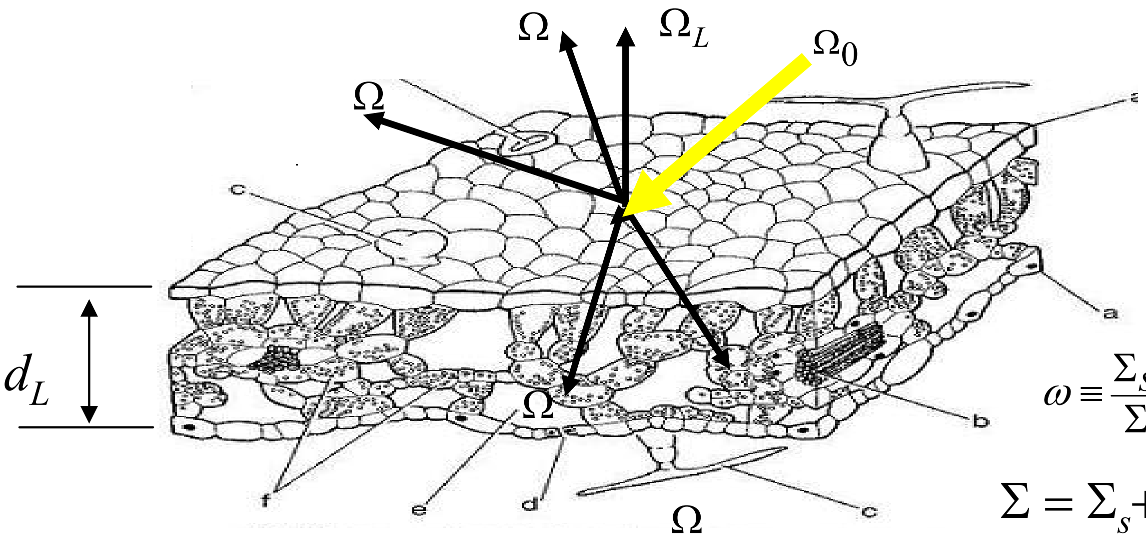

$$\omega\equiv\frac{\Sigma_S}{\Sigma}$$

$$\Sigma=\Sigma_s+\Sigma_a$$

$$\Delta_L=d_L\Sigma$$

Solution by Siewert's FN Method

Ω_0

$$I\left(0,\Omega(-\mu,\varphi);\Omega_0\right)=\frac{\omega}{4\pi}\mu_0\sum_{\alpha=0}^{L-1}a_\alpha\left(\mu_0\right)\,\phi_\alpha\left(\mu\right)$$ **BRDF**

DH-R $$\rho_L\left(\Omega_L\bullet\Omega_0\right)\equiv\frac{1}{\mu_0}\int_{2\pi^-}d\Omega\mu I\left(0,\Omega;\Omega_0\right)$$

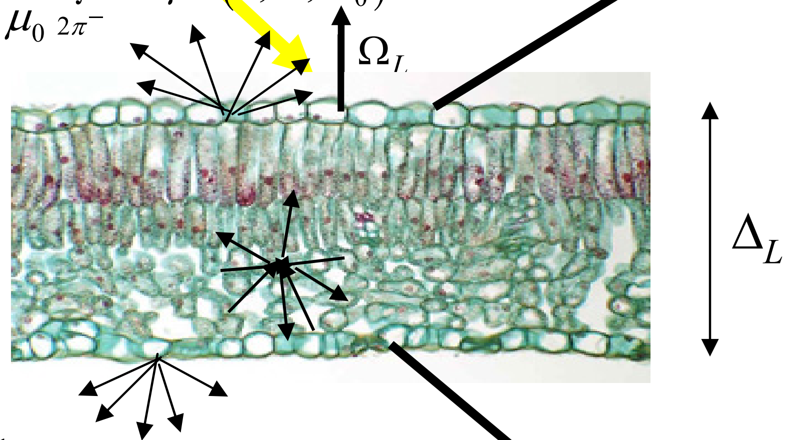

Isotropic Scattering Assumed

DH-T $$\tau_L\left(\Omega_L\bullet\Omega_0\right)\equiv\frac{1}{\mu_0}\int_{2\pi^+}d\Omega\left|\mu\right|I\left(\Delta_L,\Omega;\Omega_0\right)$$

$$I\left(\Delta_L,\Omega(\mu,\varphi);\Omega_0\right)=e^{-\Delta_L/\mu_0}\delta\left(\Omega-\Omega_0\right)+\frac{\omega}{4\pi}\mu_0\sum_{\alpha=0}^{L-1}b_\alpha\left(\mu_0\right)\,\phi_\alpha\left(\mu\right)$$ **BRTF**

Required data: Σ_a and Σ_s -- the scattering and absorption coefficients

+ Calibration of leaf scattering coefficient

LOPEX
Leaf
Data Set

Leaves of interest ← Reference leaf — Database of leaf **HH** ρ and τ

HH-R and **HH-T:** For an isotropic source

$$\rho_L(\Sigma_a,\Sigma_s)=\frac{\omega}{2}\sum_{\alpha=0}^{L-1}c_\alpha\int_0^1 d\mu\,\mu\phi_\alpha(-\mu) \qquad \tau_L(\Sigma_a,\Sigma_s)=E_2(\Delta_L)+\frac{\omega}{2}\sum_{\alpha=0}^{L-1}d_\alpha\int_0^1 d\mu\,\mu\phi_\alpha(\mu)$$

$$\begin{array}{l}\rho_L(\Sigma'_a,\Sigma_s;\lambda)=\rho_{EXP}\\ \tau_L(\Sigma'_a,\Sigma_s;\lambda)=\tau_{EXP}\end{array} \Longrightarrow \Sigma'_a(\lambda),\Sigma_s(\lambda)$$

Example: Consider a **nominal maple** canopy

d_L = 1.34mm

ρ_w = 0.723 gm/cm^3

ρ_{ch} = 38.8 μg/cm^2

Plus protein and cellulose and lignin

$\Rightarrow \Sigma'_a, \Sigma_s$

Representative maple leaf from **LOPEX**

d_L= 0.94mm

Chlorotic maple

ρ_{ch} = 0.5 x 38.8 μg/cm^2

$\Rightarrow \Sigma_a \equiv \sum_{j=1}^{J} \rho_j \sigma_j$ and Σ_s

Water Stressed maple

ρ_w =0.5 x 0.723 gm/cm^3

$\Rightarrow \Sigma_a \equiv \sum_{j=1}^{J} \rho_j \sigma_j$ and Σ_s

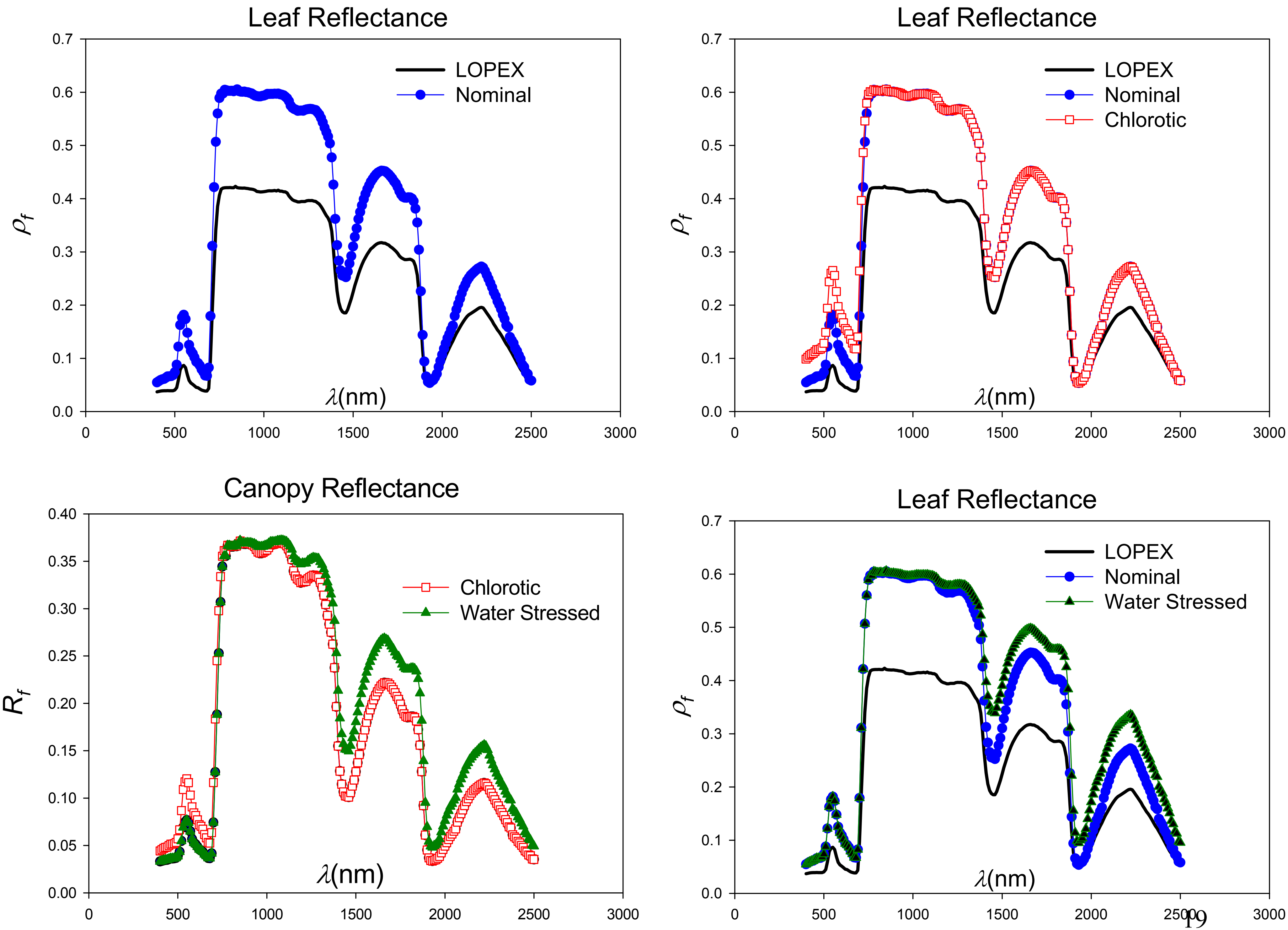

Leaf Reflectance
LOPEX
Nominal
ρ_f
λ(nm)
Leaf Reflectance
LOPEX
Nominal
Chlorotic
ρ_f
λ(nm)
Canopy Reflectance
Chlorotic
Water Stressed
R_f
λ(nm)
Leaf Reflectance
LOPEX
Nominal
Water Stressed
ρ_f
λ(nm)

+ Macroscopic diffuse leaf radiative transfer model

Leaf: Bi-Lambertian diffuse surface phase function

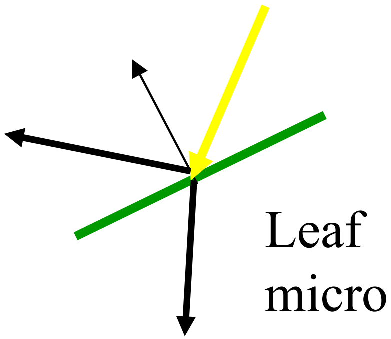

$$\gamma_D(\Omega',\Omega;\Omega_L) = \begin{cases} \dfrac{1}{\pi}\rho_L(\Omega'\cdot\Omega_L)\left|\Omega\cdot\Omega_L\right|, & (\Omega\cdot\Omega_L)(\Omega'\cdot\Omega_L) < 0 \\ \dfrac{1}{\pi}\tau_L(\Omega'\cdot\Omega_L)\left|\Omega\cdot\Omega_L\right|, & (\Omega\cdot\Omega_L)(\Omega'\cdot\Omega_L) > 0. \end{cases}$$

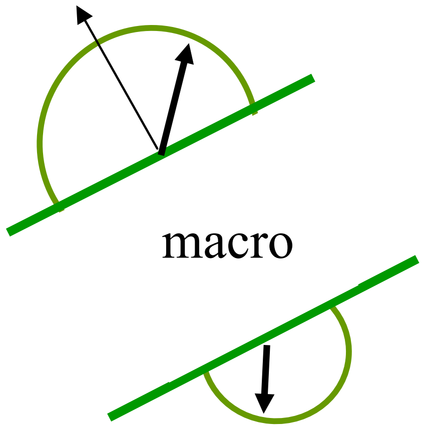

$$\rho_L(\Omega'\bullet\Omega_L) = \int_{4\pi} d\Omega\gamma_D(\Omega',\Omega;\Omega_L)$$

$$\tau_L(\Omega'\bullet\Omega_L) = \int_{4\pi} d\Omega\gamma_D(\Omega',\Omega;\Omega_L)$$

Area scattering phase function (2-angle)

$$\frac{1}{\pi}\Gamma(\Omega',\Omega) = \int_{2\pi} d\Omega_L\left|\Omega\bullet\Omega_L\right| g_L(\Omega_L)\gamma_D(\Omega',\Omega;\Omega_L).$$

$g_L(\Omega_L) \equiv$ Leaf Angle Distribution (**LAD**)

Area scattering phase function (1-angle)

$$\Gamma_D\left(\mu',\mu\right) \equiv \int_0^{2\pi} d\phi \left[\frac{1}{\pi}\Gamma_D\left(\Omega',\Omega\right)\right]$$

For **HH-** Reflectance and Transmittance

$$\gamma_D(\Omega',\Omega;\Omega_L) = \begin{cases} \frac{1}{\pi}\rho_L(\lambda)\left|\Omega\cdot\Omega_L\right|, & (\Omega\cdot\Omega_L)(\Omega'\cdot\Omega_L) < 0 \\ \frac{1}{\pi}\tau_L(\lambda)\left|\Omega\cdot\Omega_L\right|, & (\Omega\cdot\Omega_L)(\Omega'\cdot\Omega_L) > 0. \end{cases}$$

$$\Gamma_D\left(\mu',\mu\right) = 2\int_{-1}^{1} d\omega g_L(\omega) a\left(\mu',\omega\right) b(\mu,\omega)$$

Quadrature approximation

$$\Gamma\left(\mu',\mu\right) \cong \sum_{m=1}^{Lmc} g_L\left(\omega_m\right) c\left(\mu',\omega_m\right) d\left(\mu,\omega_m\right)$$

■ Leaf phase function for specular reflection and polarization

+ Specular reflection

$$\Omega' \bullet \Omega = -\cos(2\gamma)$$
$$\Omega' \bullet \Omega_L = -\cos(\gamma) \quad \Rightarrow \quad \Omega_L^*\left(\mu_L^*, \phi_L^*\right)$$
$$\Omega \bullet \Omega_L = \cos(2\gamma)$$
$$\Omega \times \Omega_L = \Omega' \times \Omega_L = \Omega' \times \Omega$$

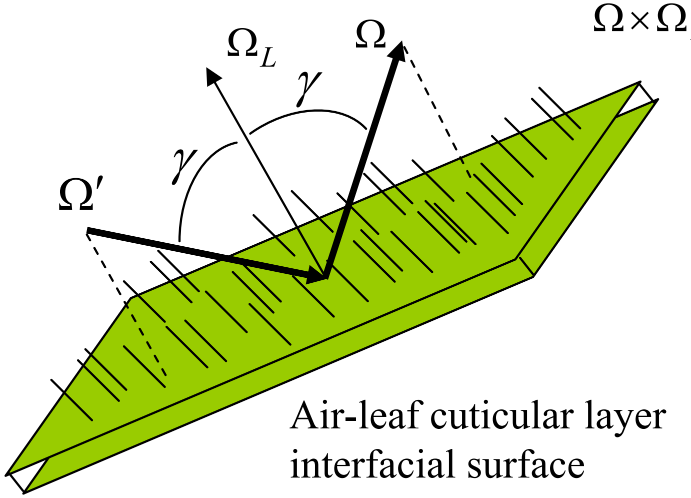

Fresnel Formula

$$F_s\left(n, \Omega' \bullet \Omega_L\right) = \frac{1}{2}\left[\frac{\sin^2(\gamma - \tilde{\gamma})}{\sin^2(\gamma + \tilde{\gamma})} + \frac{\tan^2(\gamma - \tilde{\gamma})}{\tan^2(\gamma + \tilde{\gamma})}\right]$$

$$\tilde{\gamma} \equiv \sin^{-1}\left[\frac{\sin(\gamma)}{n}\right]$$

$$\gamma_{sp}\left(\Omega', \Omega; \Omega_L\right) \equiv K\left(\kappa, \Omega' \bullet \Omega_L\right) F_s\left(n, \Omega' \bullet \Omega_L\right) \delta_2\left(\Omega \bullet \Omega_L^*\right) \qquad K\left(\kappa, \Omega' \bullet \Omega_L\right) \equiv e^{-\left[2\kappa \tan(-\Omega' \bullet \Omega)/\pi\right]}$$

Two-angle: $\displaystyle \frac{1}{\pi}\Gamma_{sp}\left(\Omega', \Omega\right) = \frac{1}{2\pi}\int_{2\pi} d\Omega_L g_L\left(\Omega_L\right)\left|\Omega' \bullet \Omega_L\right| \gamma_{sp}\left(\Omega', \Omega; \Omega_L\right) = \frac{1}{8\pi} g_L\left(\mu_L^*\right) K(\kappa, \gamma) F_s(n, \gamma)$

One-angle: $\displaystyle \Gamma_{sp}\left(\mu', \mu\right) = \frac{1}{4\pi}\int_0^{\pi} d\omega g_L\left(\mu_L^*\left[\cos(\omega)\right]\right) K\left(\kappa, \gamma\left[\cos(\omega)\right]\right) F_s\left(n, \gamma\left[\cos(\omega)\right]\right)$

+ Phase function for the linearly polarized component

-- Experimental evidence indicates that polarization originates predominately at the leaf surface from specular reflection.

-- Use the vector transport equation to describe the intensity and the linearly polarized component.

Phase function for the linearly polarized component: the mathematical model

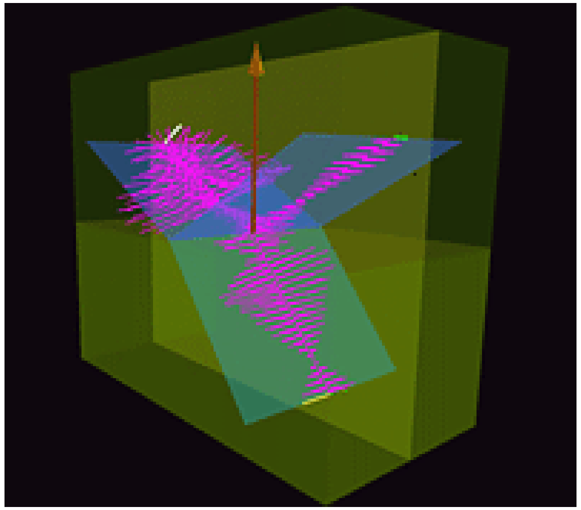

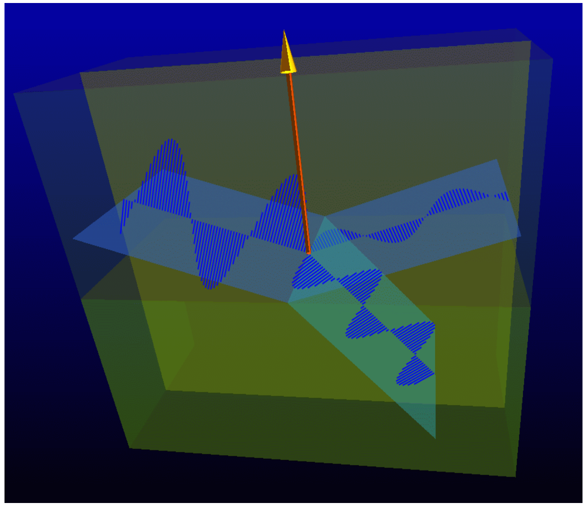

$$\rho_{\parallel} = \frac{1}{2}\left[\frac{\sin^2(\gamma-\tilde{\gamma})}{\sin^2(\gamma+\tilde{\gamma})}\right]$$

Intensity: $\rho_s = F_s(n,\gamma) = \frac{1}{2}[\rho_{\parallel} + \rho_{\perp}]$

$$\rho_{\perp} = \frac{1}{2}\left[\frac{\tan^2(\gamma-\tilde{\gamma})}{\tan^2(\gamma+\tilde{\gamma})}\right]$$

Second Stokes Component: $\rho_Q = F_Q(n,\gamma) = \frac{1}{2}[\rho_{\parallel} - \rho_{\perp}]$

$$\underline{L}(\lambda) \equiv \begin{bmatrix} 1 & 0 \\ 0 & \cos(2\lambda) \end{bmatrix}$$

$$\underline{T}(n,\gamma) = \begin{bmatrix} F_s(n,\gamma) & F_Q(n,\gamma) \\ F_Q(n,\gamma) & F_s(n,\gamma) \end{bmatrix}$$

Phase Function: $\underline{\Gamma}(\mu',\mu) =$

$$= \frac{1}{4\pi}\int_0^{\pi} d\omega g_L(\mu_L^*)\underline{L}(-\lambda)\bullet$$

$$\bullet K(\kappa,\gamma(\Omega'\bullet\Omega))\underline{T}(n,\gamma(\Omega'\bullet\Omega))\underline{L}(\lambda').$$

The Radiative Transport Algorithm with Leaf Polarization

■ The Vector Transport Equation

$$\vec{I}(\tau,\mu) \equiv \begin{bmatrix} I(\tau,\mu) \\ Q(\tau,\mu) \end{bmatrix} \qquad \left[\mu \underline{I} \frac{\partial}{\partial \tau} + G(\mu)\underline{I}\right]\vec{I}(\tau,\mu) = \int_{-1}^{1} d\mu' \underline{\Gamma}(\mu',\mu)\vec{I}(\tau,\mu')$$

+BC

$$\vec{I}(\tau,\mu) = \vec{I}_0(\tau,\mu) + \vec{I}_c(\tau,\mu)$$

Uncollided component: $\vec{I}_0(\tau,\mu) = \begin{bmatrix} 1 \\ 0 \end{bmatrix} e^{-\tau/\xi}\delta(\mu-\mu_0)\Theta(\tau/\xi)$ $\qquad \xi \equiv \mu/G(\mu)$

Collided component:

$$\left[\mu \underline{I} \frac{\partial}{\partial \tau} + G(\mu)\underline{I}\right]\vec{I}_c(\tau,\mu) =$$

$$= \int_{-1}^{1} d\mu' \underline{\Gamma}(\mu',\mu)\vec{I}_c(\tau,\mu') + \underline{\Gamma}(\mu_0,\mu)\begin{bmatrix} 1 \\ 0 \end{bmatrix} e^{-\tau/\xi_0}$$

Intercept function:

$$G(\Omega) = \frac{1}{2\pi}\int_{2\pi+} d\Omega_L \left|\Omega \bullet \Omega_L\right| g_L(\Omega_L)$$

$$\vec{I}_c(0,\mu) = 0$$

$$\vec{I}_c(\Delta,-\mu) = 2\rho_T\left[\mu_0 e^{-\tau/\xi_0} + \int_0^1 d\mu'\mu' I_c(\Delta,\mu')\right]\begin{bmatrix} 1 \\ p_T \end{bmatrix}$$

Degree of polarization of Target

■ The SN/Romberg Algorithm for Intensity

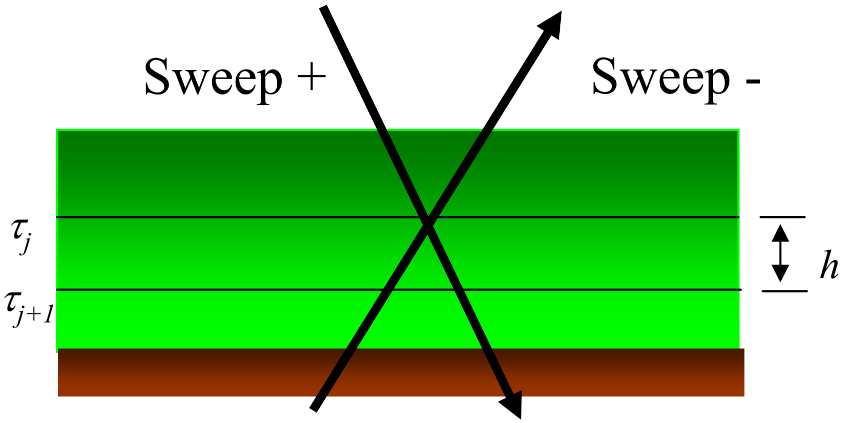

Discretized spatial domain

Discretizations:

$$P_{N/2}(\pm\mu_m)=0,\quad m=1,N/2$$

$$h\equiv\ \Delta/N_h$$

Romberg iteration:

$$\int_h dx g(x)=\sum_{k=1}^{K}\alpha_k g_k+O(h^K)$$

$$I_{c,j,m}^{Exact}=I_{c,j,m}+\sum_{k=2}^{\infty}\beta_k h^k$$

$$\mu_m\left[I_{c,j+1,m}-I_{c,j,m}\right]+G_m\int_h d\tau I_{c,m}(\tau)=$$

$$=\sum_{m'=1}^{N}\omega_{m'}\Gamma(\mu_{m'},\mu_m)\int_h d\tau I_{c,m'}(\tau)+$$

$$+\ \xi_0\Gamma_{0,m}\left[e^{-\tau_j/\xi_0}-e^{-\tau_{j+1}/\xi_0}\right],$$

$$T_m^- I_{c,j+1,m}-T_m^+ I_{c,j,m}=q_{j,m}+$$

$$+\frac{h}{2}\sum_{m'=1,\neq m}^{N/2}\omega_{m'}\Gamma_{m',m}\begin{bmatrix}I_{c,j+1,m'}+\\ +I_{c,j,m'}\end{bmatrix}+$$

$$+\frac{h}{2}\sum_{m'=N/2+1,\neq m}^{N}\omega_{m'}\Gamma_{m',m}\begin{bmatrix}I_{c,j+1,m'}+\\ +I_{c,j,m'}\end{bmatrix}$$

■ Numerical implementation and convergence

Evaluation of area scattering phase functions

$$\Gamma\left(\mu', \mu\right) = \int_0^{\pi} d\omega f\left(\cos(\omega)\right) = \sum_{m=1}^{Lmc} \omega_m f_m$$

Iteration Strategy--

(1) Increment **SN** order and quadrature order **Lmc**

(2) Perform **SN** sweeps to convergence

(3) Monitor reflectance and transmittance for both components

(4) Apply Wynn-epsilon acceleration

$$\varepsilon_{-1}^{(n)} = 0, \quad \varepsilon_{0}^{(n)} = S_n$$

$$\varepsilon_{k+1}^{(n)} = \varepsilon_{k}^{(n+1)} + \left[\varepsilon_{k}^{(n+1)} - \varepsilon_{k}^{(n)}\right]^{-1}$$

(5) Go to (1) until (4) converges

■ Qualification and Demonstration (Zenith Sun)

Comparison of **LCM2/LCM2P (LAI** = 1, ρ_T = 0.1)

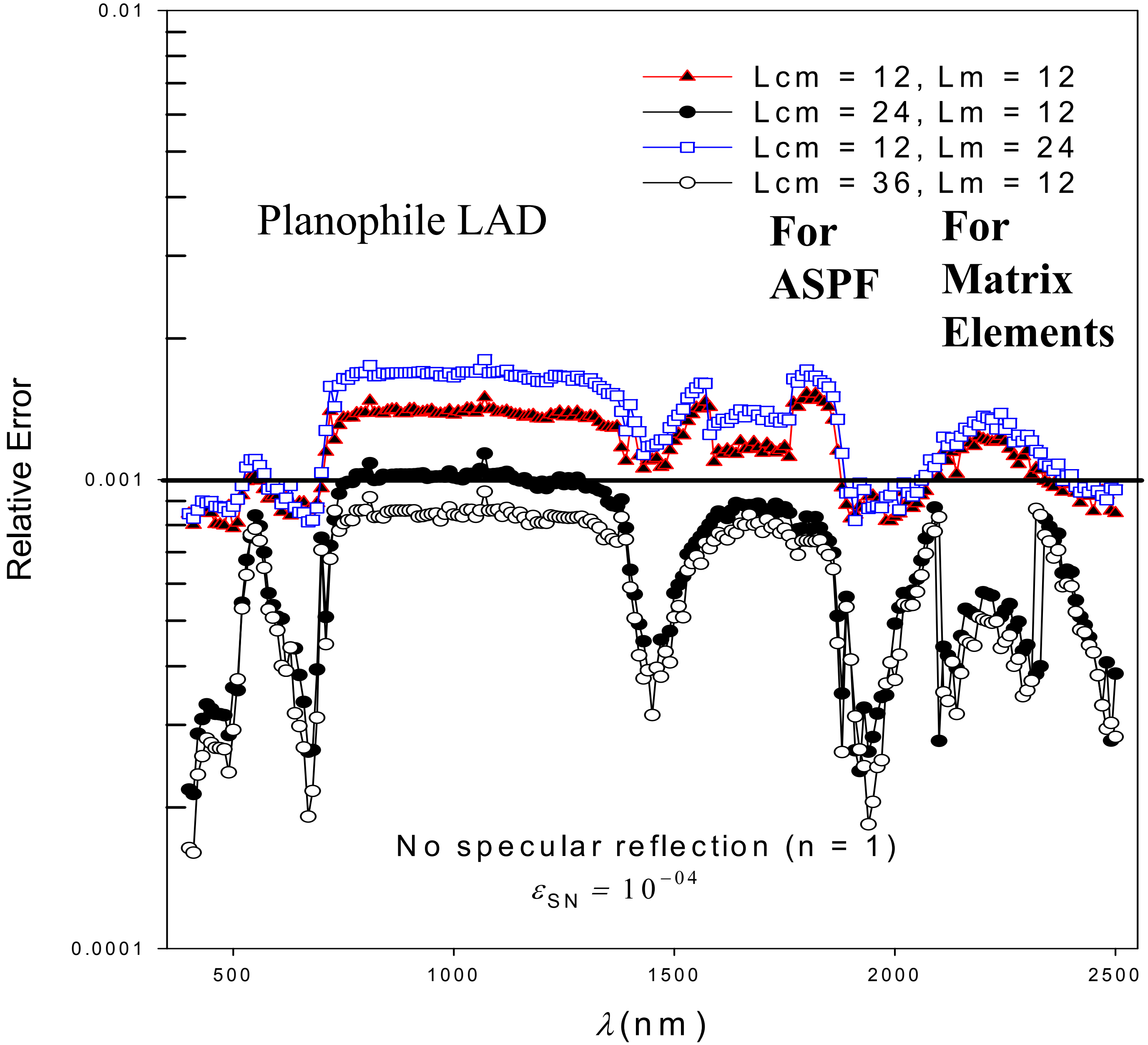

Comparison of FN and SN/Romberg for Planophile LAD (1)

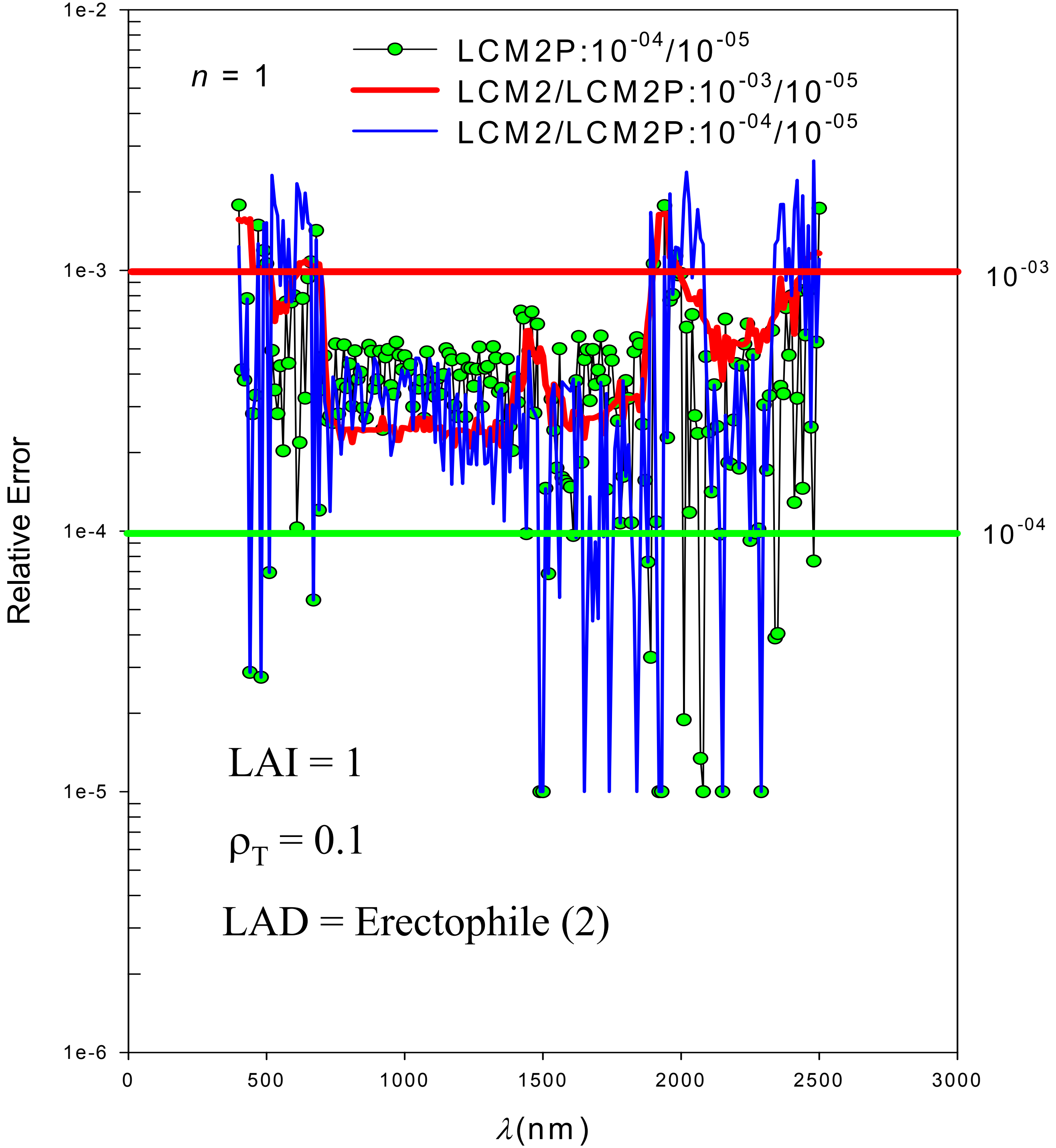

Comparison of FN and SN/Romberg for Erectophile LAD

Table 1
Convergence of the W-ε Acceleration (N_0 = 10)

Lm	*Lmc*	*W-ε*	*Rfn*	*Error W-ε*	*Error Rfn*
22	10	3.6810E-02	3.6810E-02	2.6166E+01	1.0000E+00
24	12	3.6868E-02	3.6868E-02	1.5579E-03	1.5579E-03
26	14	3.6903E-02	3.6903E-02	9.6828E-04	9.6828E-04
28	16	3.6927E-02	3.6927E-02	6.5138E-04	6.5138E-04
30	18	3.6944E-02	3.6944E-02	4.5973E-04	4.5973E-04
32	20	3.6957E-02	3.6957E-02	3.3706E-04	3.3706E-04
34	22	3.6966E-02	3.6966E-02	2.5506E-04	2.5506E-04
36	24	3.6973E-02	3.6973E-02	1.8287E-04	1.8287E-04
38	26	3.6977E-02	3.6977E-02	1.1872E-04	1.1872E-04
40	28	3.6980E-02	3.6980E-02	6.8486E-05	6.8486E-05
42	30	3.6981E-02	3.6981E-02	4.2281E-05	4.2281E-05
44	32	3.6983E-02	3.6983E-02	3.3926E-05	3.3926E-05
46	34	3.6984E-02	3.6984E-02	3.5482E-05	3.5482E-05
48	36	3.6986E-02	3.6986E-02	4.0690E-05	4.0690E-05
50	38	3.6987E-02	3.6987E-02	4.7207E-05	4.7207E-05
52	40	3.6986E-02	3.6989E-02	4.2763E-05	5.3886E-05
54	42	3.6989E-02	3.6991E-02	8.0632E-05	4.9856E-05
56	44	3.6989E-02	3.6992E-02	1.1775E-06	3.0001E-05
58	46	3.6996E-02	3.6993E-02	1.9800E-04	1.9641E-05
60	48	3.6989E-02	3.6994E-02	1.9303E-04	1.4928E-05
62	50	3.6966E-02	3.6994E-02	6.1240E-04	1.4725E-05
64	52	3.6993E-02	3.6995E-02	7.1229E-04	1.5901E-05
66	54	3.7002E-02	3.6995E-02	2.6683E-04	1.7624E-05
68	56	3.6999E-02	3.6996E-02	1.0612E-04	1.4997E-05
70	58	3.6999E-02	3.6996E-02	3.9680E-07	1.1253E-05
72	60	3.6999E-02	3.6997E-02	1.0864E-06	8.8883E-06
74	62	3.7000E-02	3.6997E-02	3.1928E-05	8.1139E-06
76	64	3.6997E-02	3.6997E-02	7.8482E-05	7.8789E-06
78	66	3.6999E-02	3.6998E-02	4.4057E-05	8.6515E-06
80	68	3.7000E-02	3.6998E-02	4.2742E-05	7.9577E-06
82	70	3.7000E-02	3.6998E-02	2.0422E-07	6.2885E-06
84	72	3.7000E-02	3.6998E-02	7.1298E-07	5.3577E-06
86	74	3.7000E-02	3.6998E-02	1.0642E-05	4.8736E-06
88	76	3.7000E-02	3.6999E-02	8.9489E-06	4.7407E-06
90	78	3.7001E-02	3.6999E-02	1.5724E-05	4.9800E-06
92	80	3.7001E-02	3.6999E-02	6.6756E-06	4.6481E-06
94	82	3.7001E-02	3.6999E-02	1.7446E-06	3.8941E-06
96	84	3.7000E-02	3.6999E-02	2.6794E-05	3.4720E-06
98	86	3.7001E-02	3.6999E-02	2.3889E-05	3.1392E-06
100	88	3.7001E-02	3.6999E-02	8.5448E-07	3.1088E-06
102	90	3.7001E-02	3.7000E-02	1.5302E-06	3.1535E-06

Variation with Index of Refraction

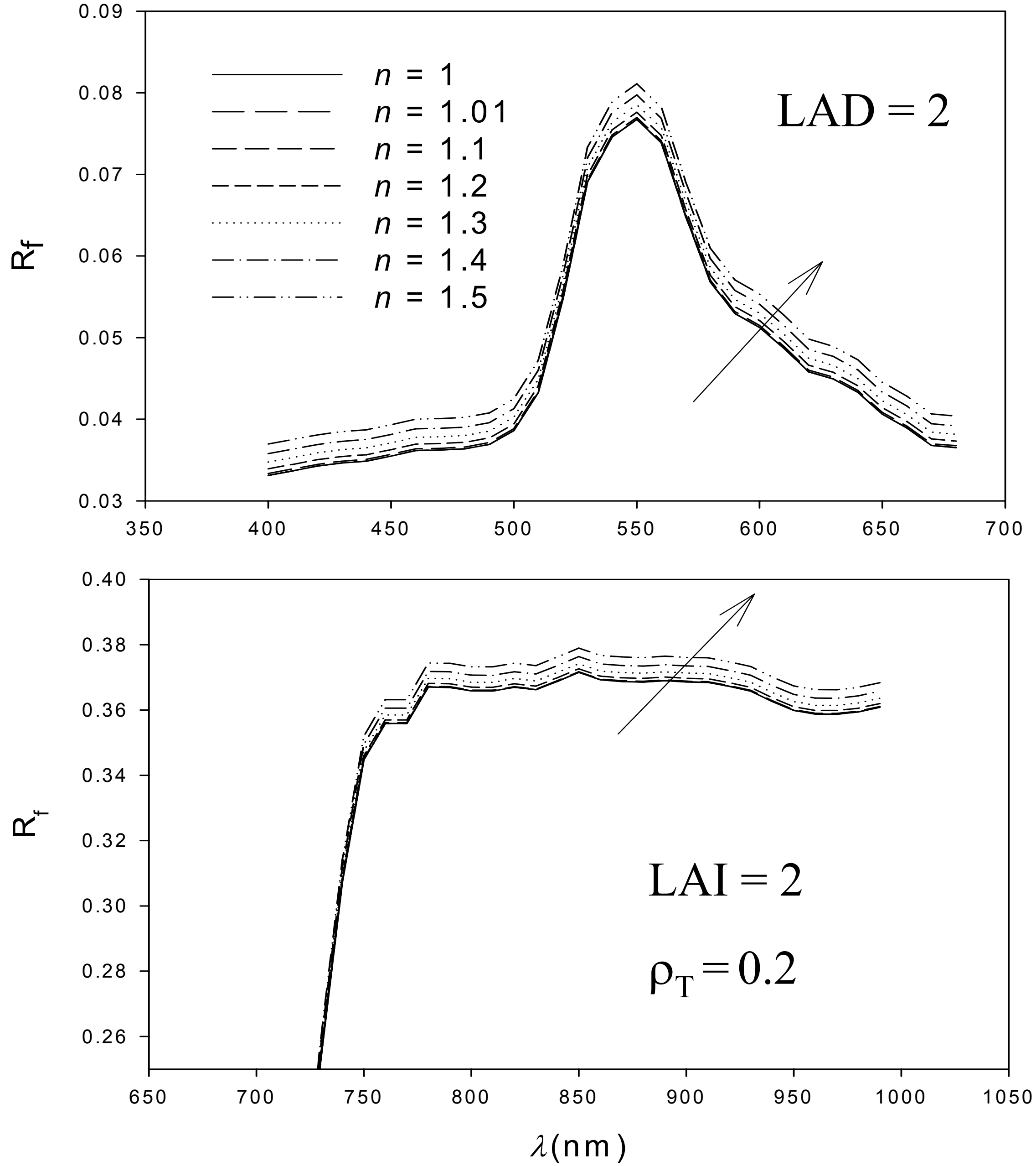

Canopy reflectance with specular leaf reflection for an unpolarized target

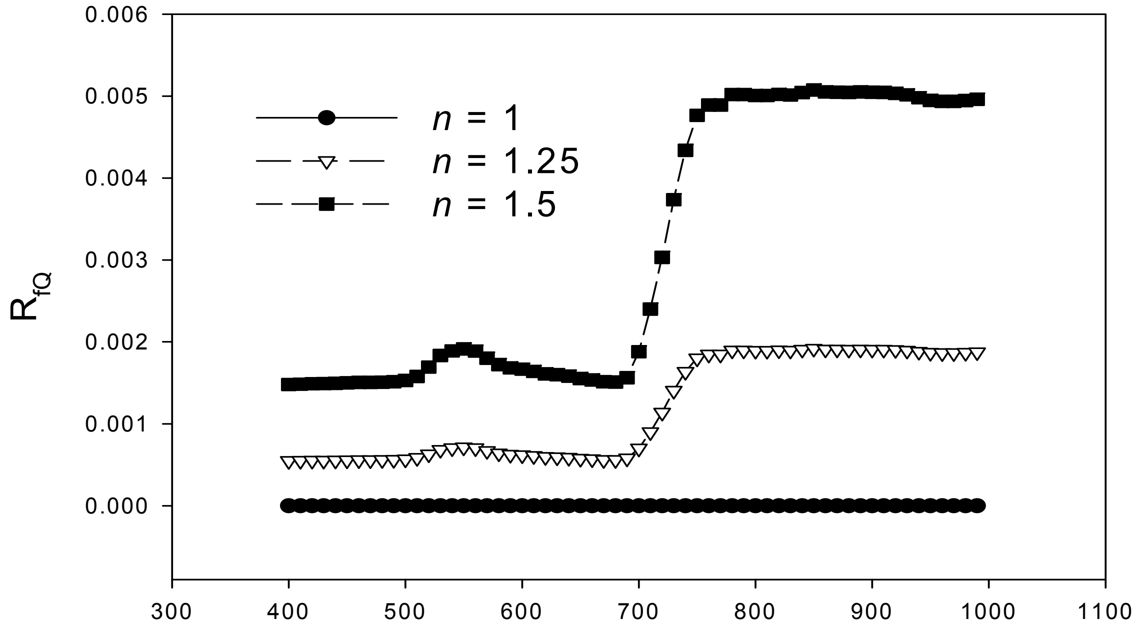

Linearly polarized reflectance R_{fQ} and degree of polarization (Dp0) for an unpolarized target

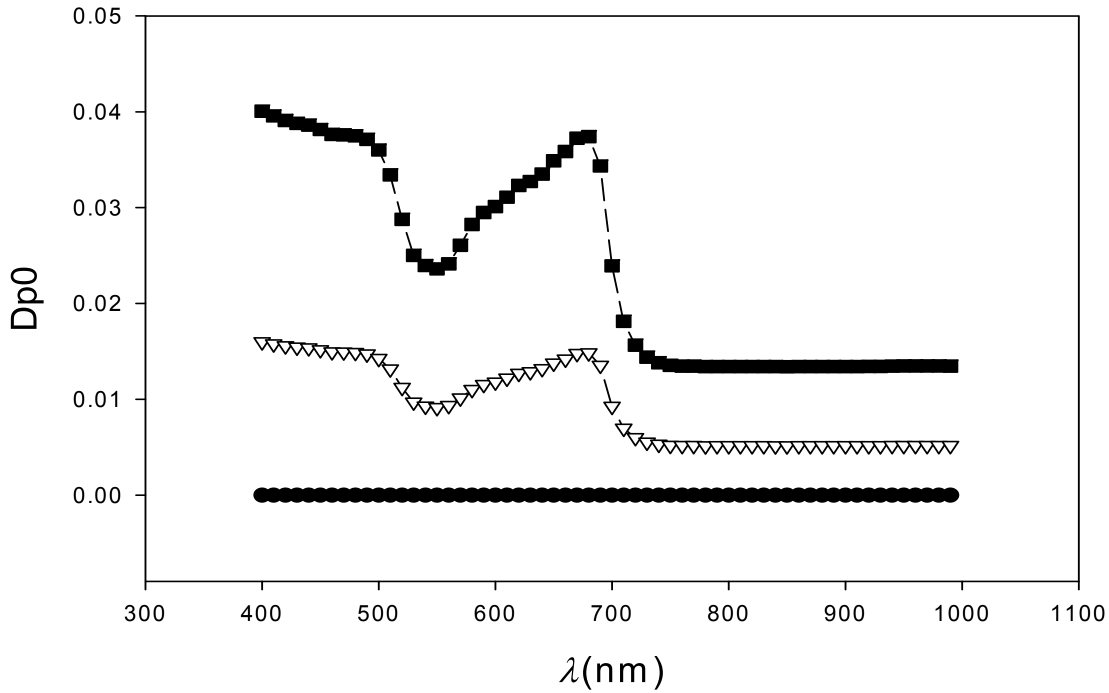

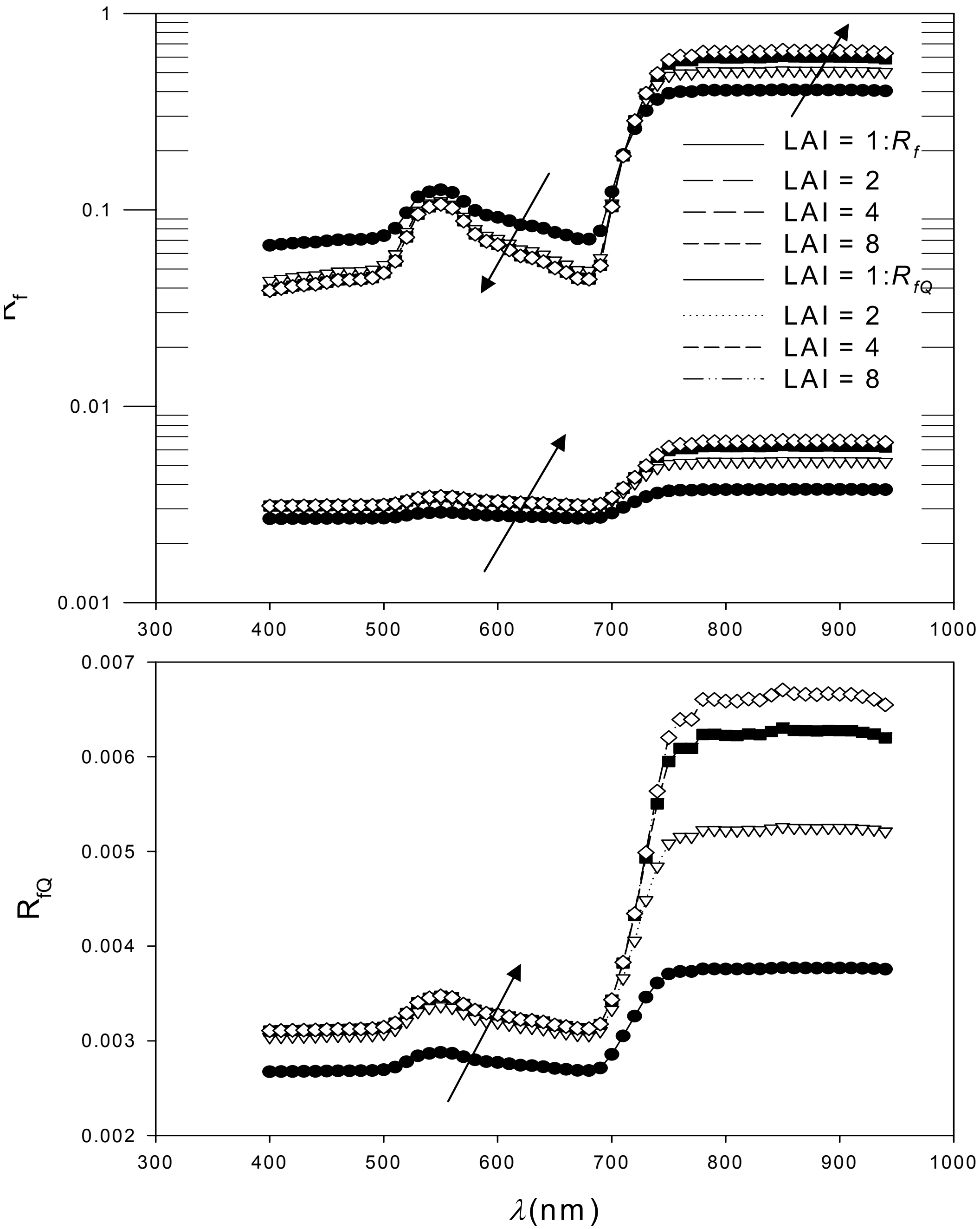

Variation of LAI over unpolarized target
LAD = Planophile

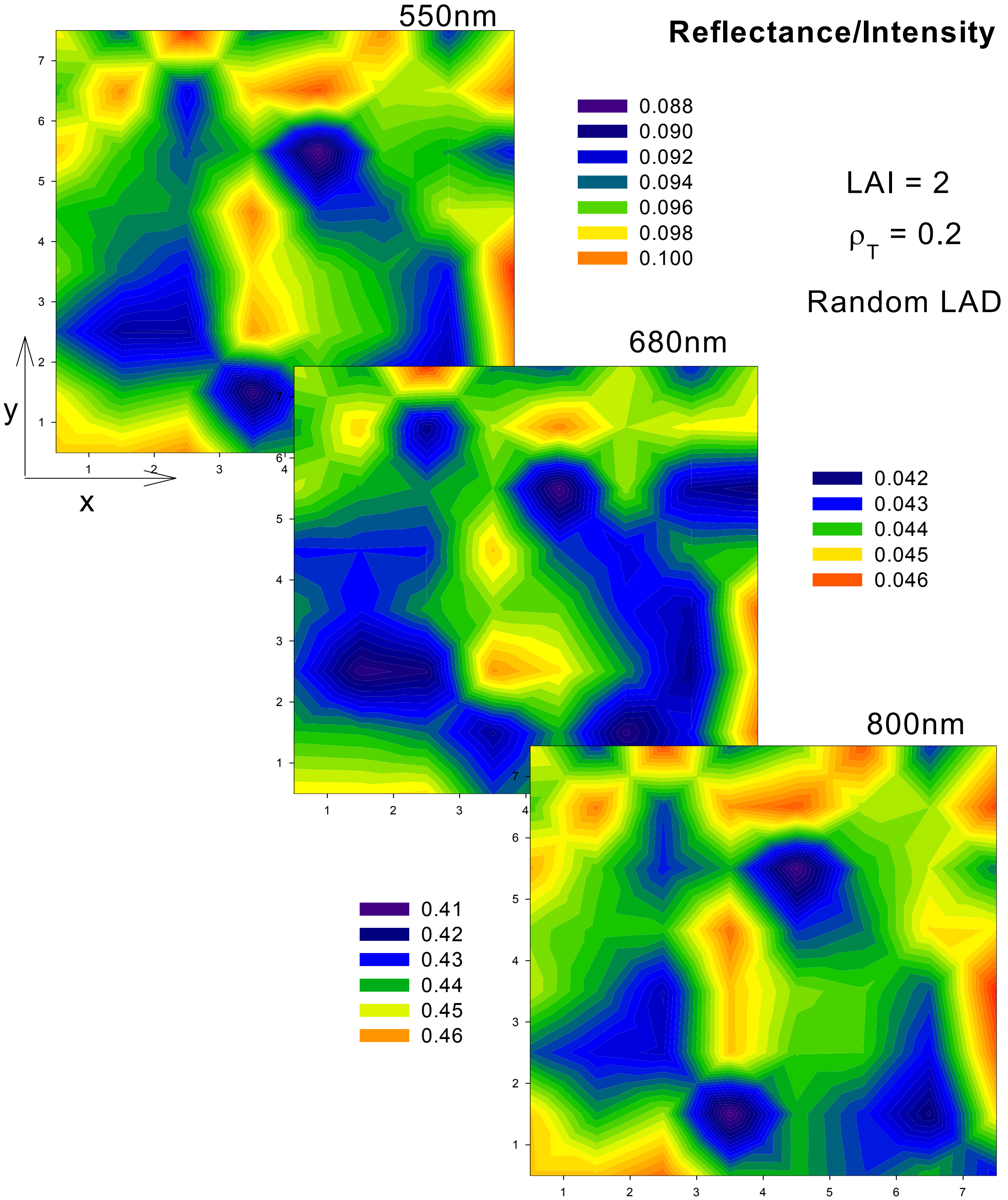
Reflectance/Intensity
550nm
0.088
0.090
0.092
0.094
0.096
0.098
0.100
LAI = 2
ρ_T = 0.2
Random LAD
680nm
0.042
0.043
0.044
0.045
0.046
800nm
0.41
0.42
0.43
0.44
0.45
0.46
y
x

Degree of Linear Polarization (Dp0) at TOC

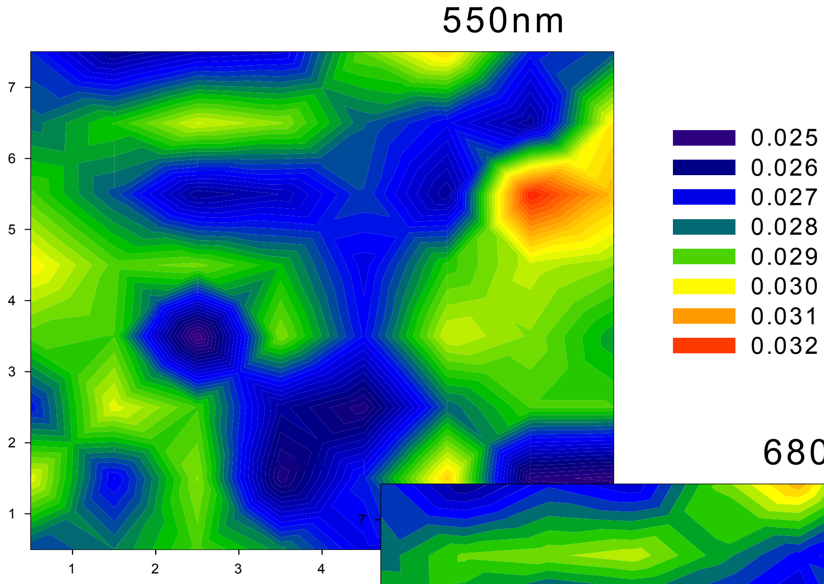

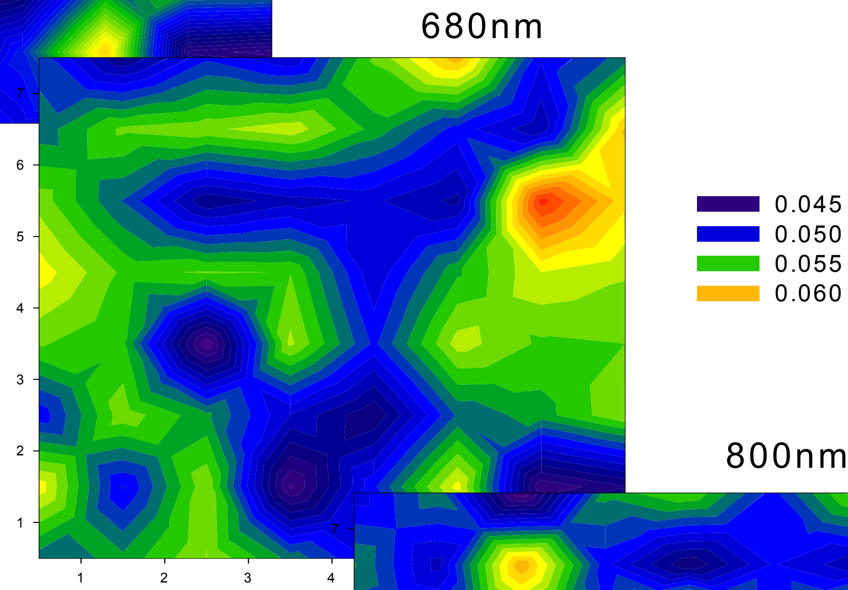

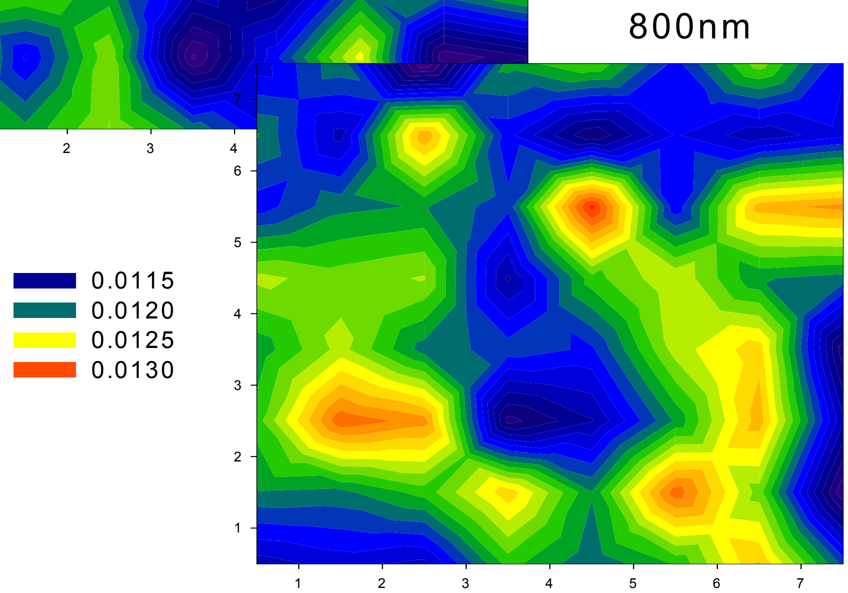

Reflectance/I

LAI = 2

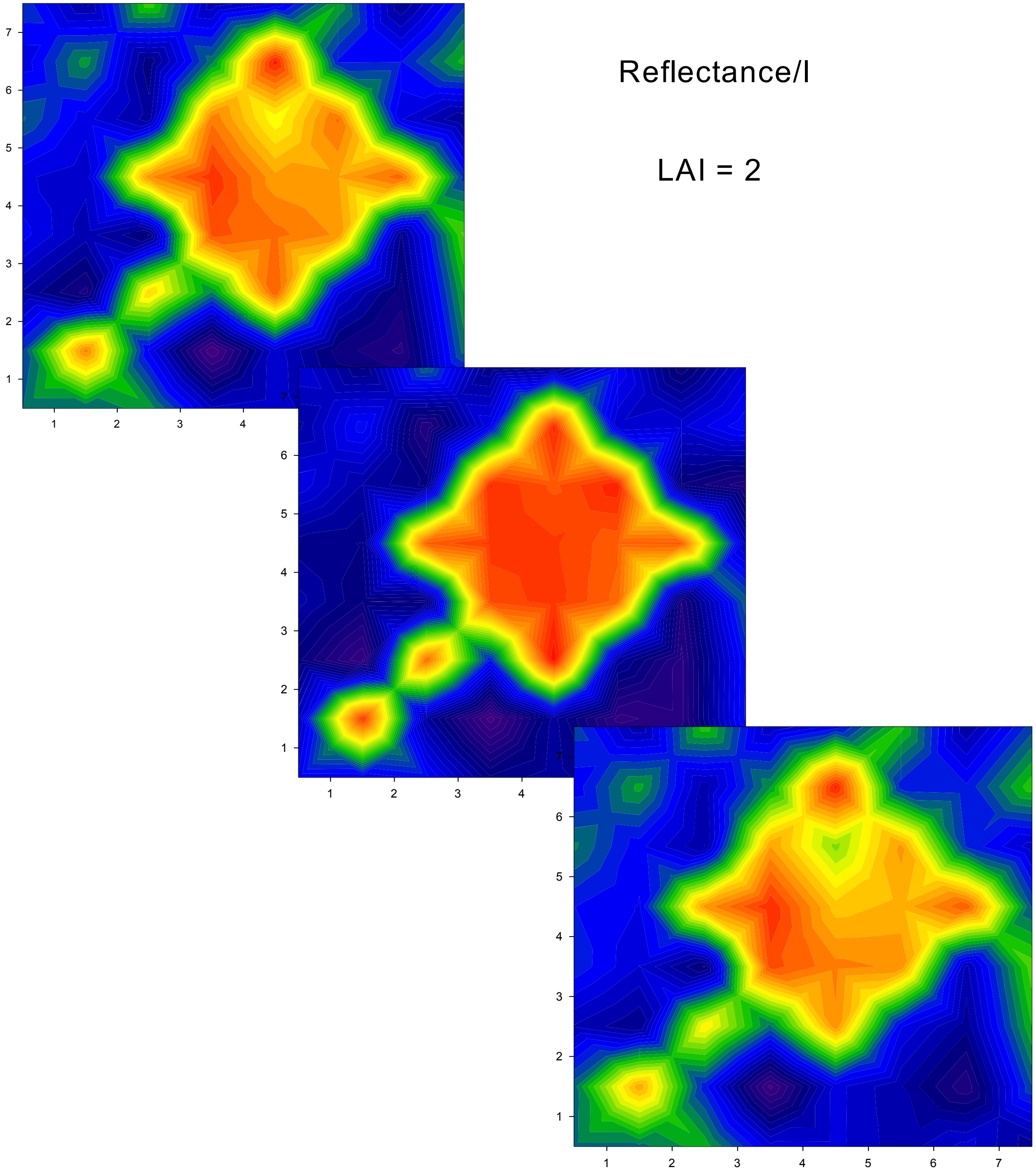

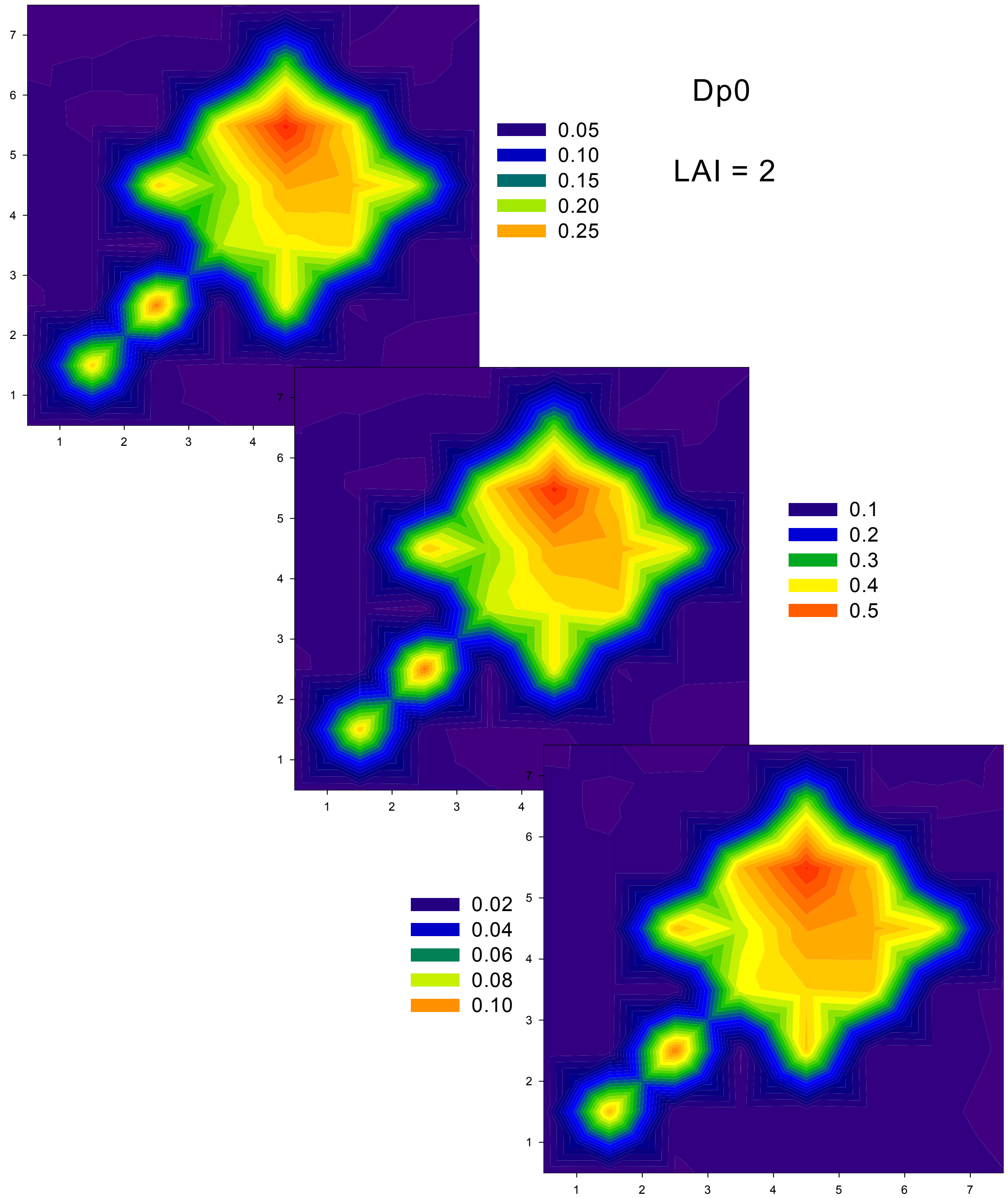
Dp0
LAI = 2
0.05
0.10
0.15
0.20
0.25
0.1
0.2
0.3
0.4
0.5
0.02
0.04
0.06
0.08
0.10

Reflectance/I

LAI = 4

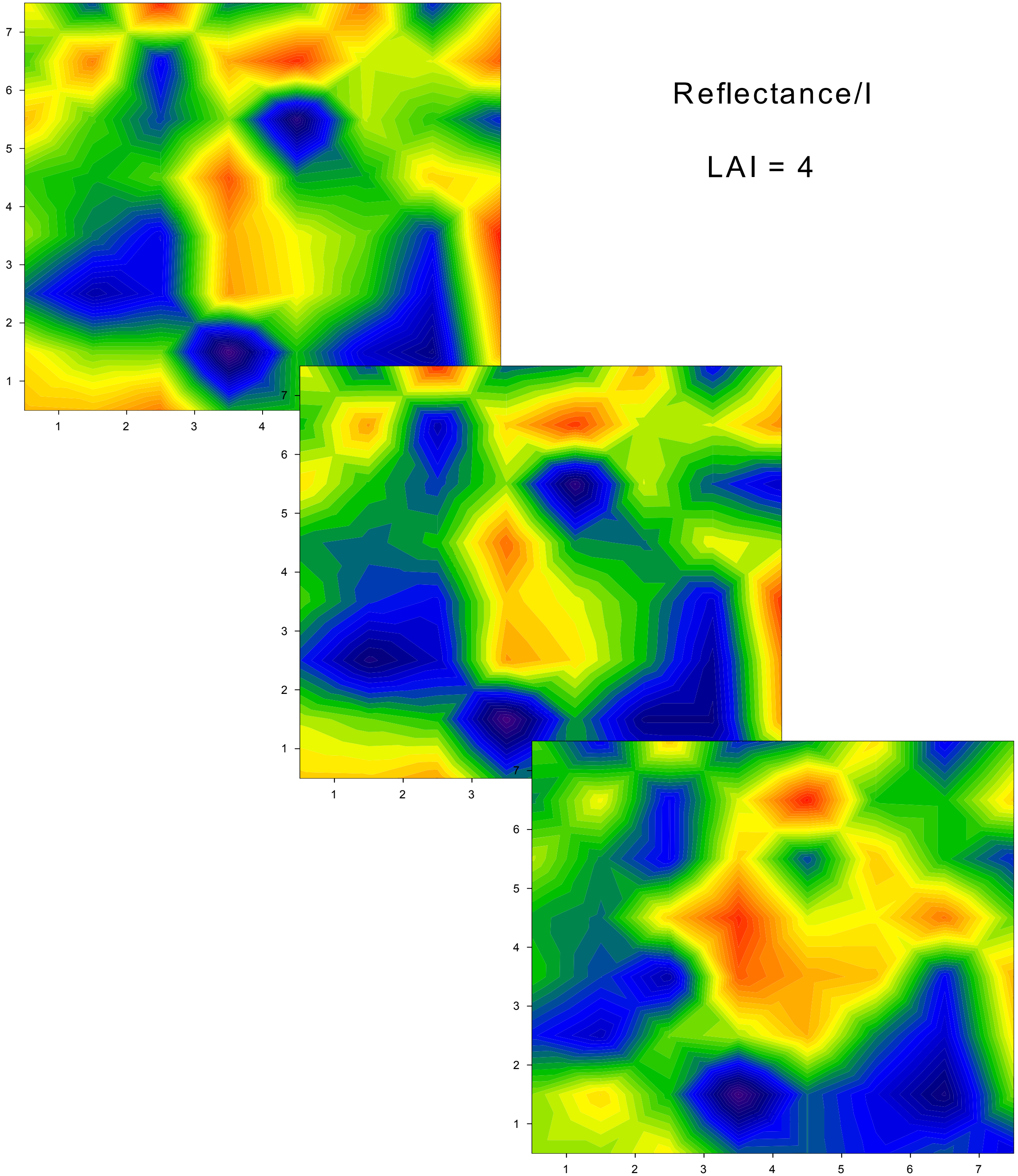

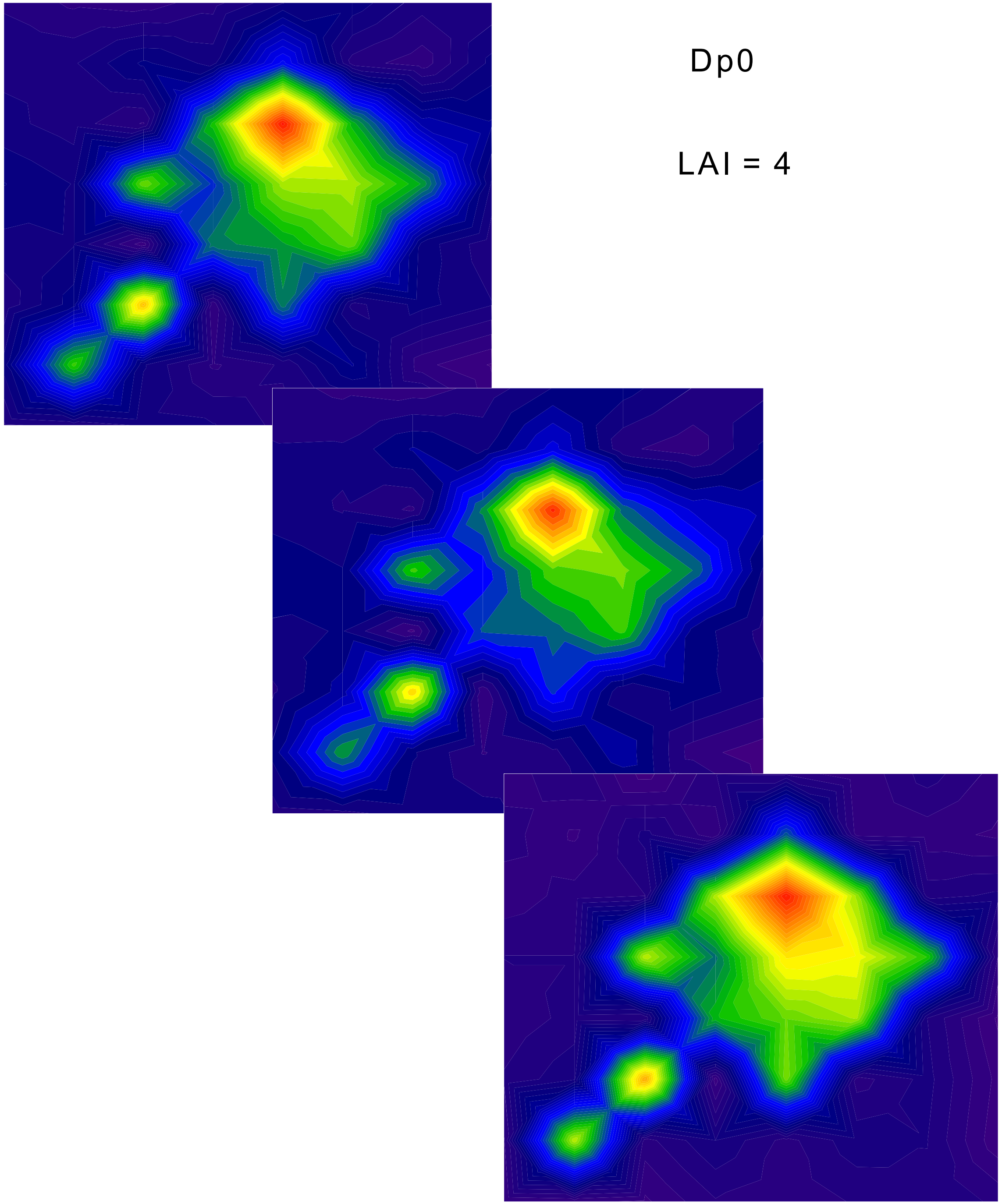

Dp0

LAI = 4

Reflectance/I

LAI = 6

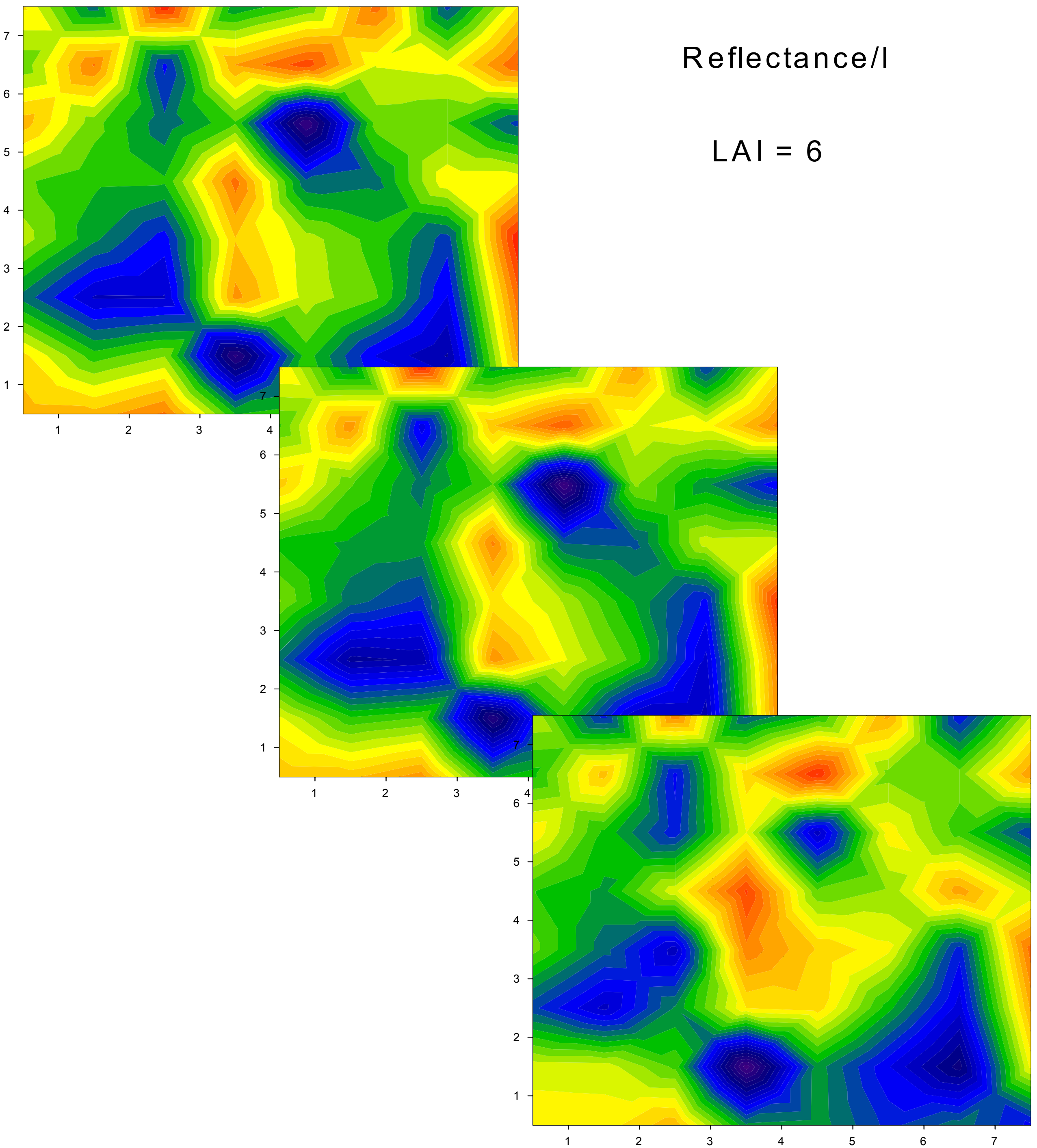

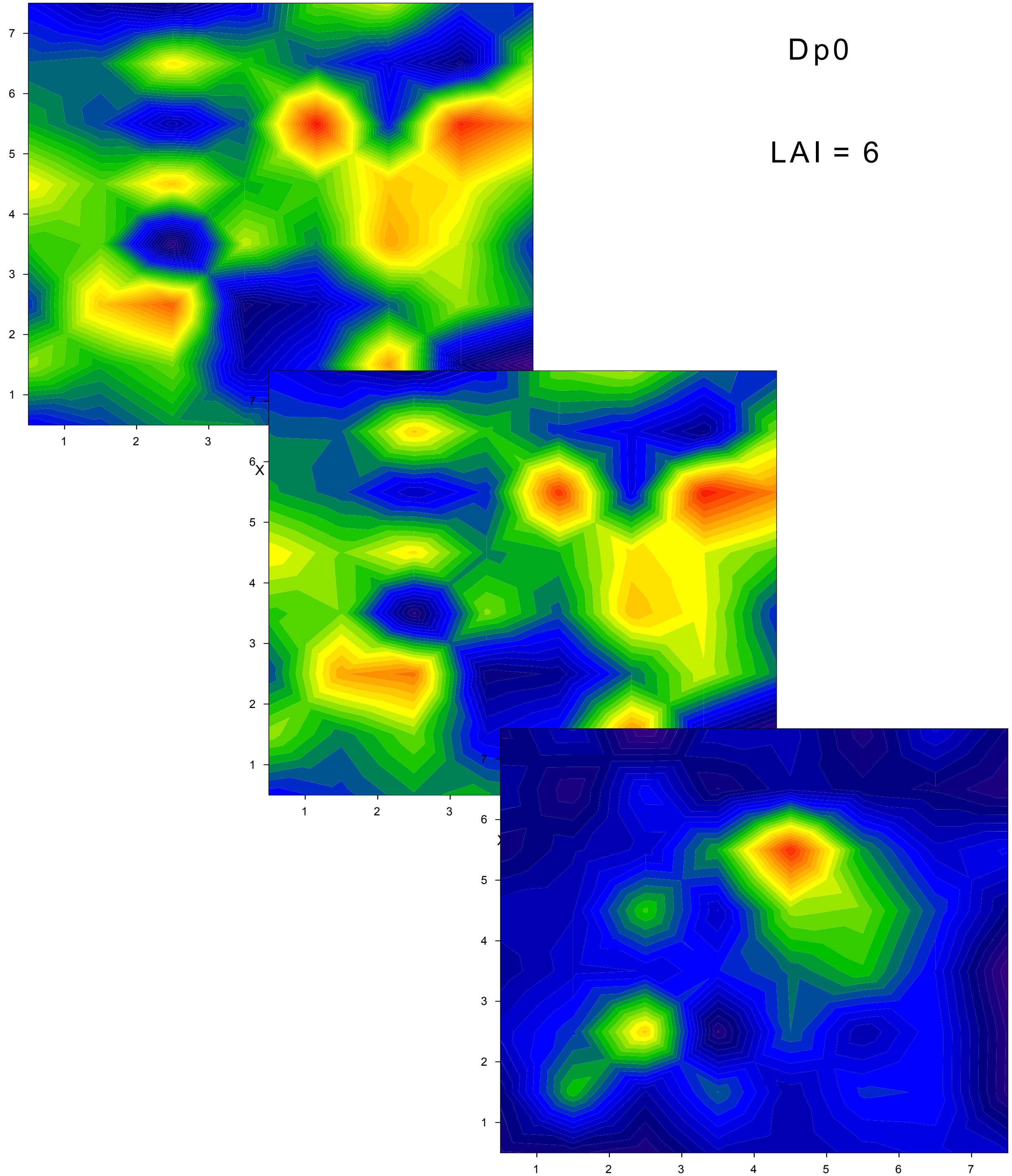

Dp0

LAI = 6

Reflectance/Intensity

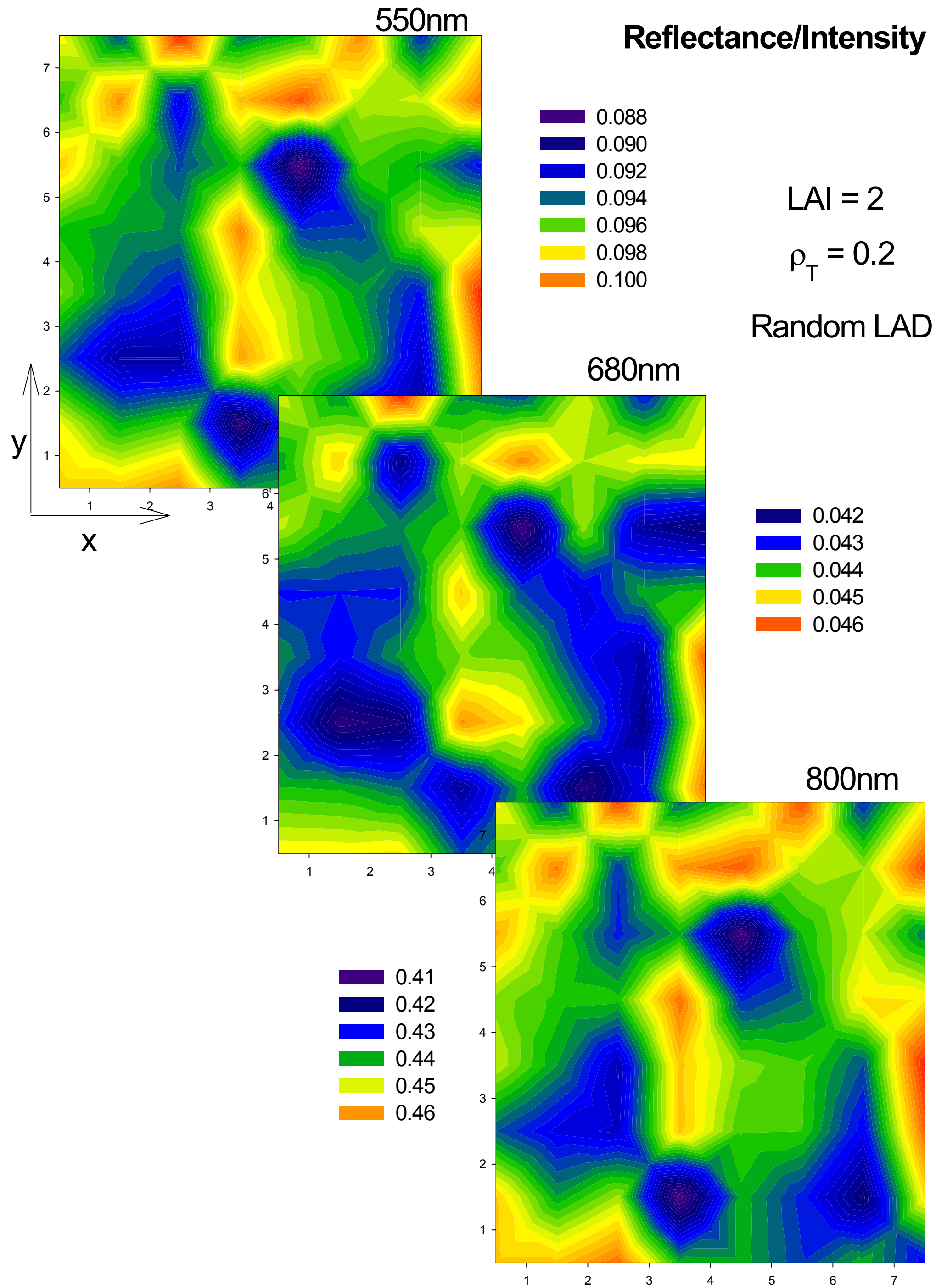

LAI = 2

$\rho_T = 0.2$

Random LAD

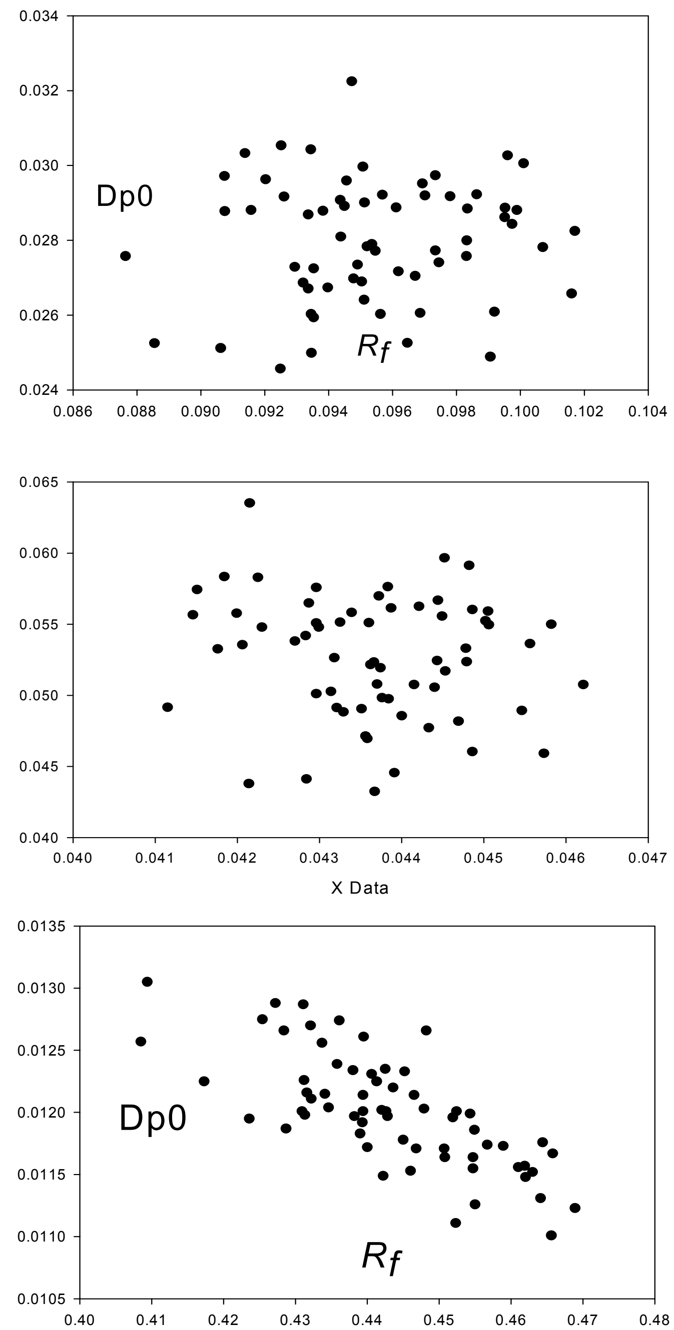

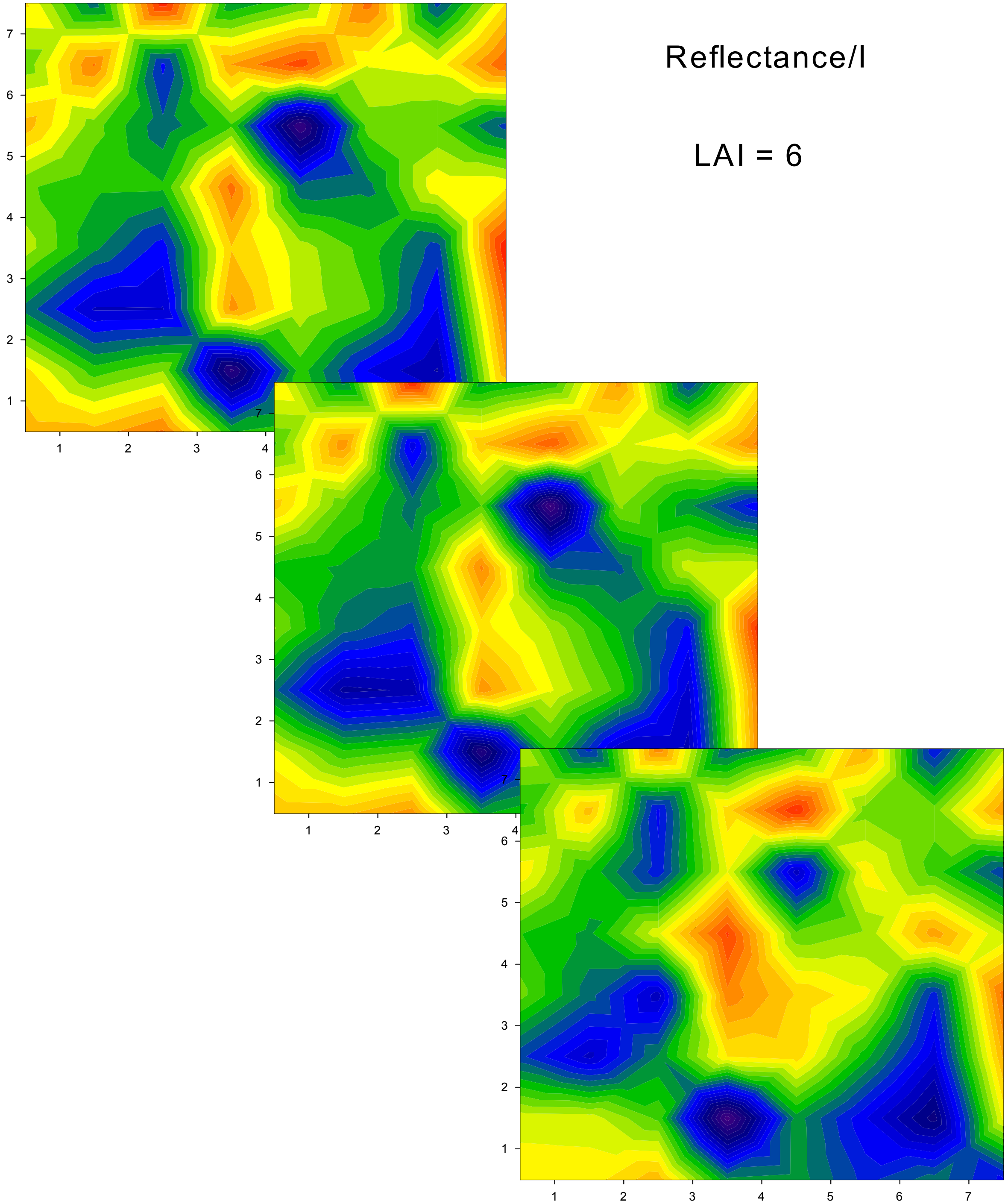

Reflectance/I

LAI = 6

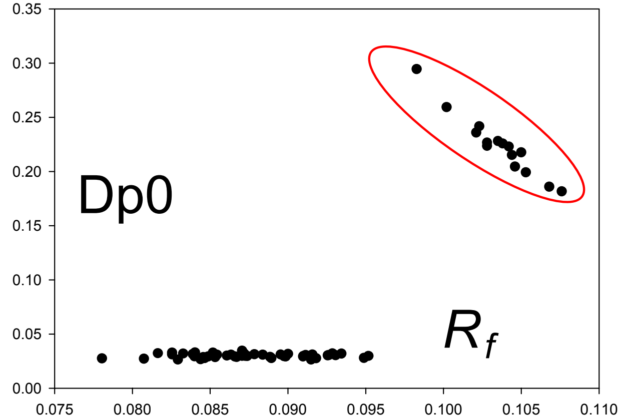

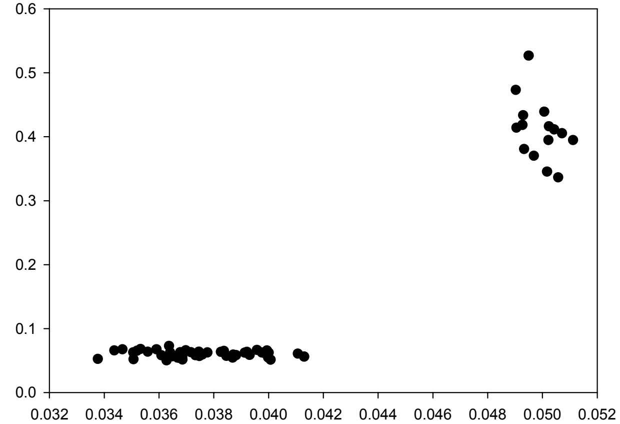

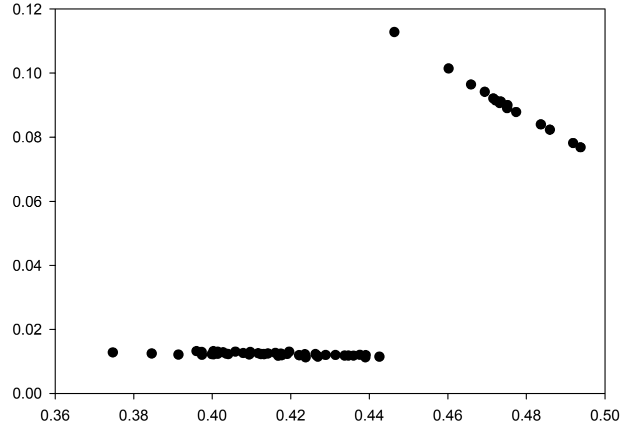

4 Background Polarizations

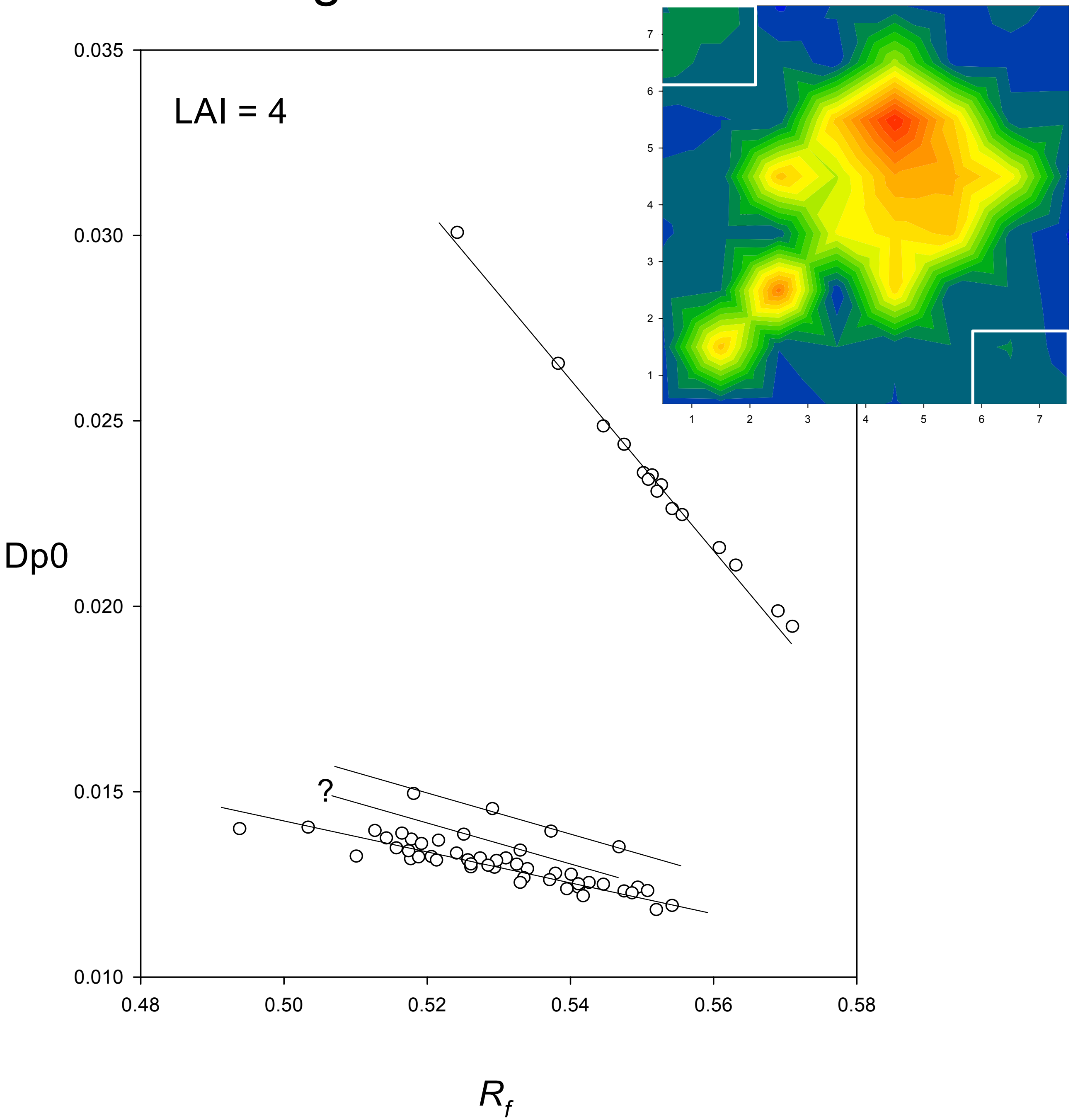

MODEL-BASED NEURAL NETWORK ALGORITHM FOR COFFEE RIPENESS PREDICTION USING HELIOS UAV AERIAL IMAGES

R. Furfaro[a], B. Ganapol[a]*, L. Johnson[b], S. Herwitz[b]

a: Aerospace Mechanical Engineering Dept, University of Arizona, AZ
b: NASA AMES Reseach Center, Moffet Field, CA

***: Speaker**

SPIE 11th International Symposium Remote Sensing
Bruges, 19-22 September 2005

UAVs FOR PRECISION AGRICULTURE:

- UAV: Unpioleted Aerial Vehicle (Air Tower)
- Helios and Pathfinder-plus prototypes
- NASA technology transfer concept
- New way of doing agriculture

CLARK UNIVERSITY NASA Ames Research Center TAAC AeroVironment KAUAI COFFEE COMPANY California State University Monterey Bay The University of Arizona

NASA COFFEE PROJECT: "The Vision"

- Searching for "heavenly " coffee through UAVs: Helping the farmers to find the best harvesting strategy using remote sensing
- 1st mission for technology proof of concept flew in Oct '02
- Our group is involved in image processing
- Research and practical issue: Can we create an intelligent reliable algorithm to predict the percentage of ripe (yellow) cherries in the field?

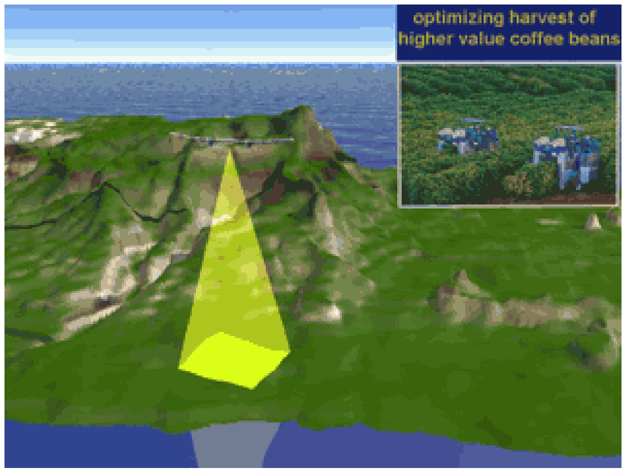

SOLUTION: Model Based Neural Network

- Design a Neural Network trained to learn the percentage of ripe cherries in the field
- The algorithm is based on a true radiative transport model
- The algorithm is to be put on the on-board microprocessor to elaborate airborne images
- Ripe percentages sent to the ground for real-time prediction

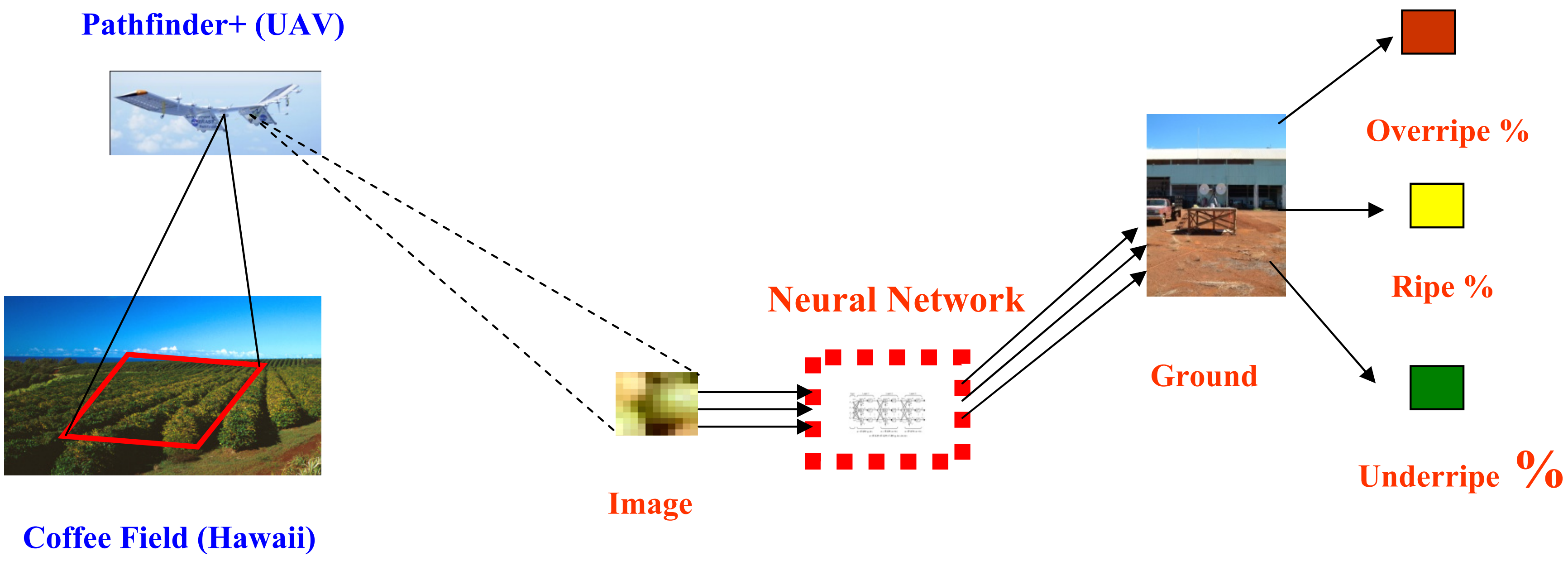

MODELING THE RADIATIVE REGIME IN PLANT CANOPIES:LCM2

Goal: generation of a true radiative transport model to simulate the radiative field in vegetation canopies

Approach:

- First principles application: Balance of photons
- Two levels of description: Leaf and Canopy model (nested models)
- Biochemistry included as key element affecting vegetation optics
- Connection of the models via leaf optical properties

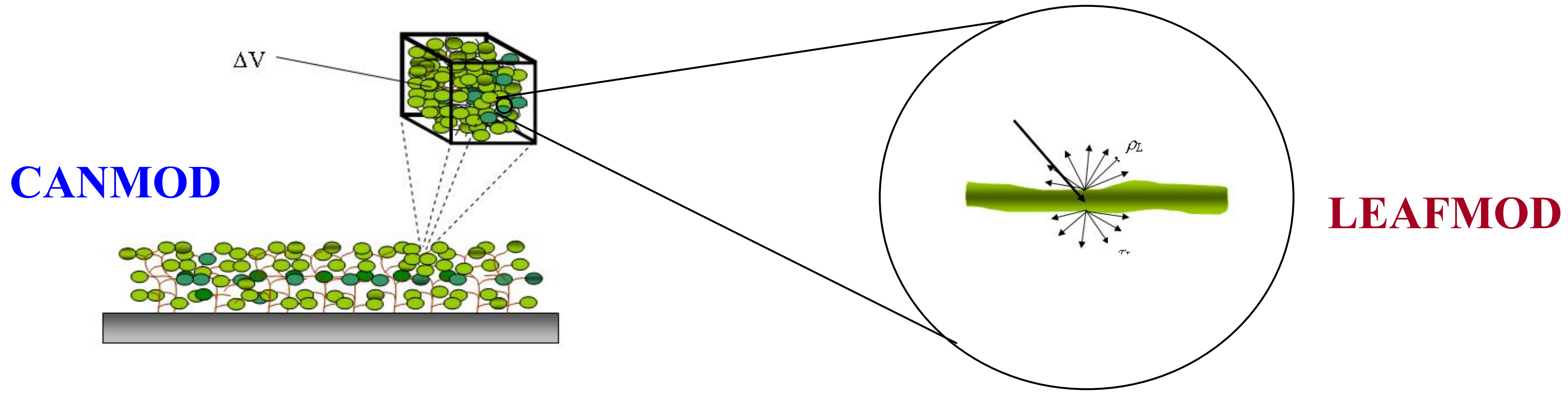

CANOPY GOVERNING EQUATION

Balance of photons in the phase space: Plane symmetry

$$\left[\mu\frac{\partial}{\partial\tau}+G(\mu)\right]I(\tau,\Omega)=\frac{1}{\pi}\int_{4\pi}d\Omega'\Gamma(\Omega',\Omega)I(\tau,\Omega')$$

In-scattering

Streaming

Out-scattering

Boundary Conditions

$$I(0,\Omega)=F_L(\Omega),\mu>0$$

$$I(\Delta,\Omega)=F_R(\Omega)=\frac{r_s}{\pi}\int_{2\pi}d\Omega'|\mu'|I(\tau,\Omega'),\mu<0$$

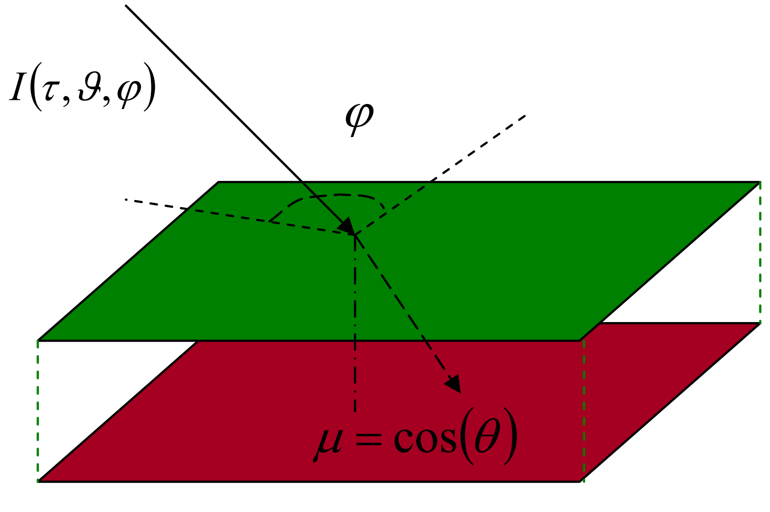

Model output: Reflectance at Top of Canopy

$$R_f=\frac{1}{\pi}\int_{2\pi}d\Omega'|\mu'|I(0,\Omega'),\mu<0$$

Leaf/Canopy Model: LCM2 FLOWCHART

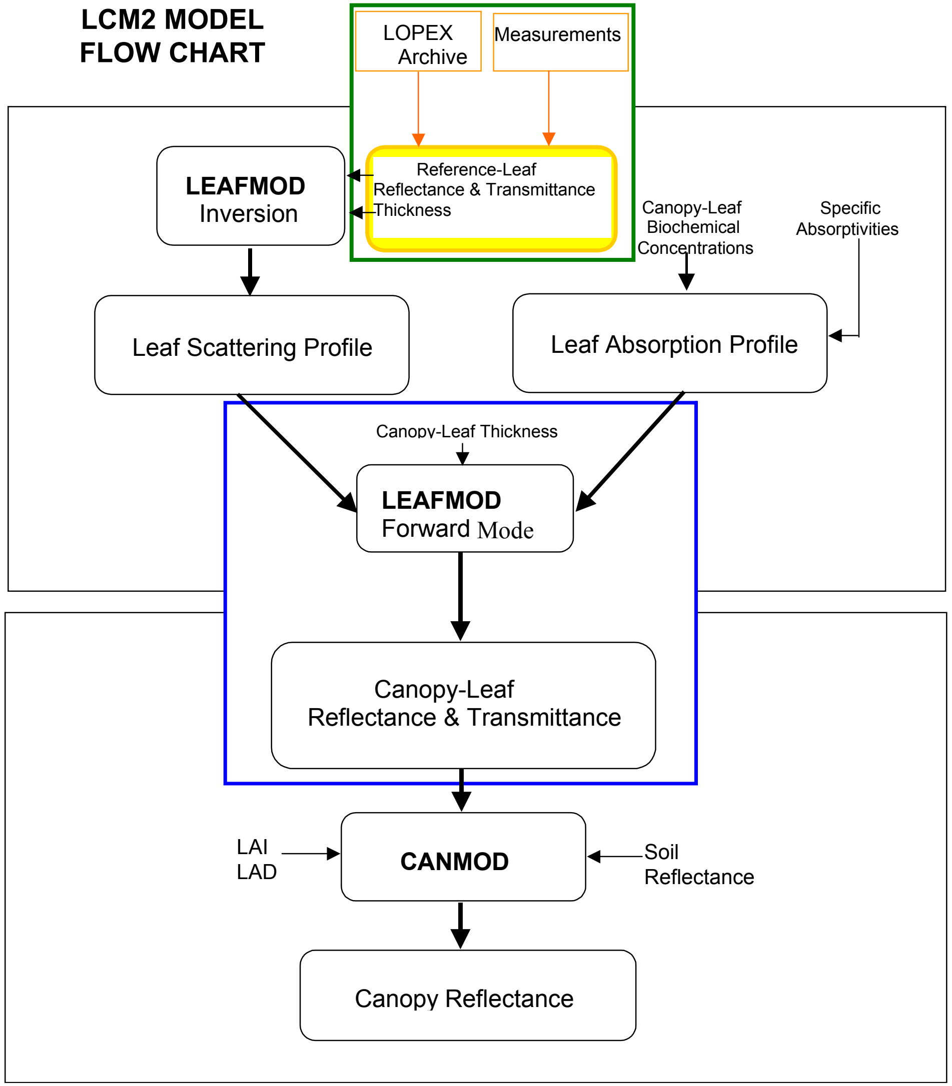

Neural Networks (NNs) Overview

- **NNs are composed by elements operating in parallel. They are biologically inspired to nervous systems**
- **NNs function depends on the way elements are connected**
- **NNs “learn”: Learning can be supervised or not**
- **NNs applications: Classification, Pattern recognitions, control systems etc.**

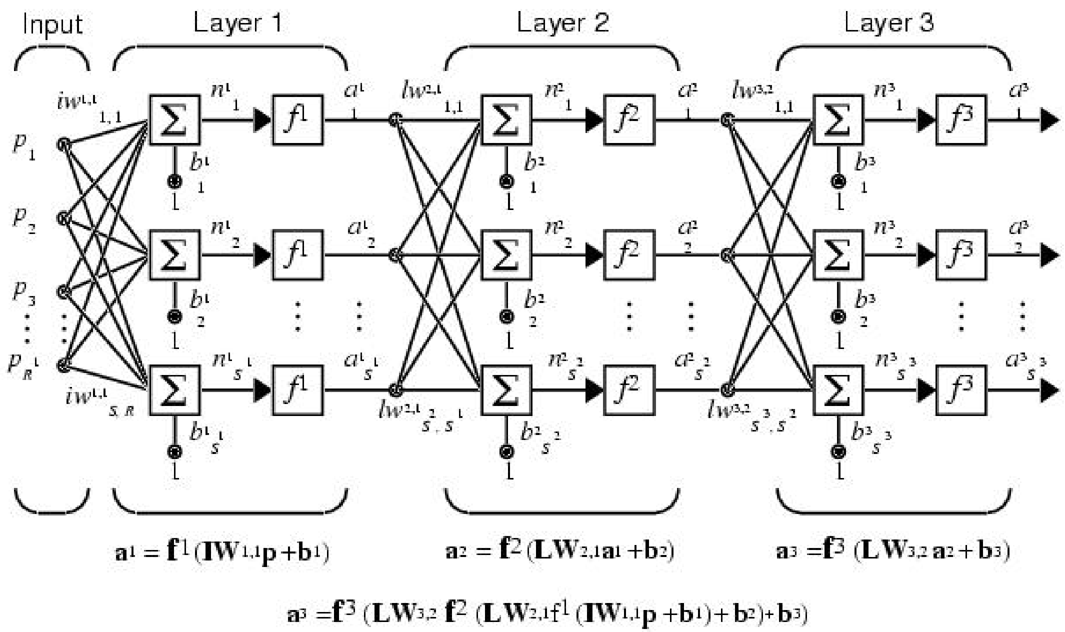

Model Based NN: Design and Training

- LCM in the forward mode

$$R_f = f(D_{ch}, D_w, D_p, D_{lc}, Sp, LAI, LAD, SR, RC\%, GC\%, YC\%, M\%, \lambda)$$

- LCM in the inverse mode

$$[M\%, RC\%, GC\%, YC\%] = f(D_{ch}, D_w, D_p, D_{lc}, Sp, LAI, LAD, SR, R_f, \lambda)$$

- Reduced inverse problem: Design issues

  How many neurons in the hidden layer?
  How many points in the training set?

- Neural Network performance:

  Learn the training set
  Generalizes well

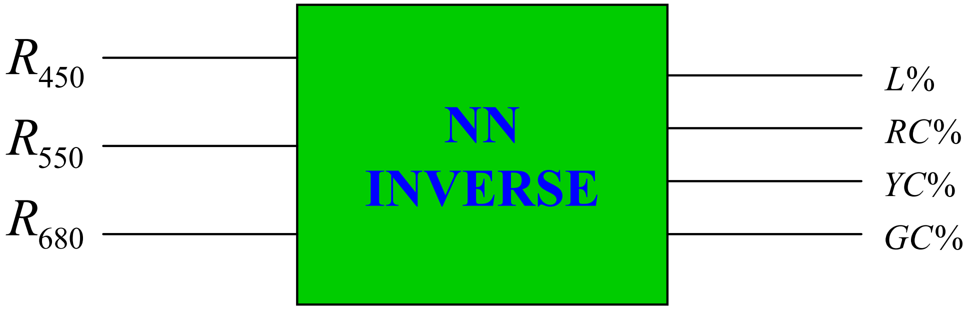

- Advantage: Model knowledge allow us to generate as many points as needed
- Disadvantage: Model may not be in the domain of experiment

Training Results and Regression analysis

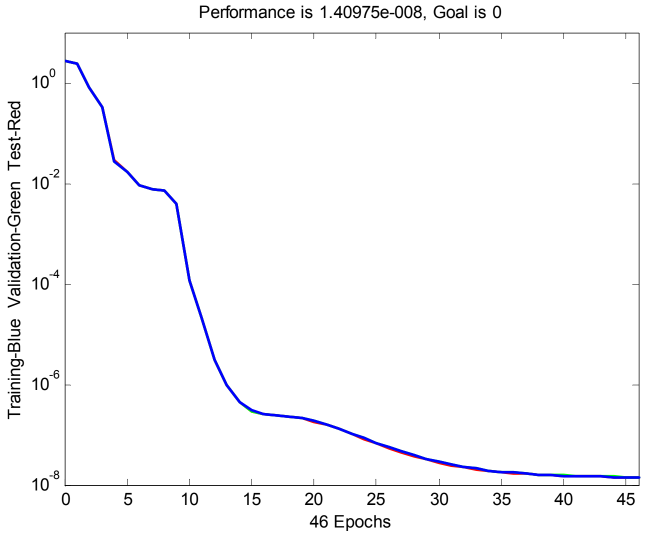

- Network Trained in **"Batch mode"**
- Training goal for the **error function 10^{-7}**
- Early **stopping** not observed

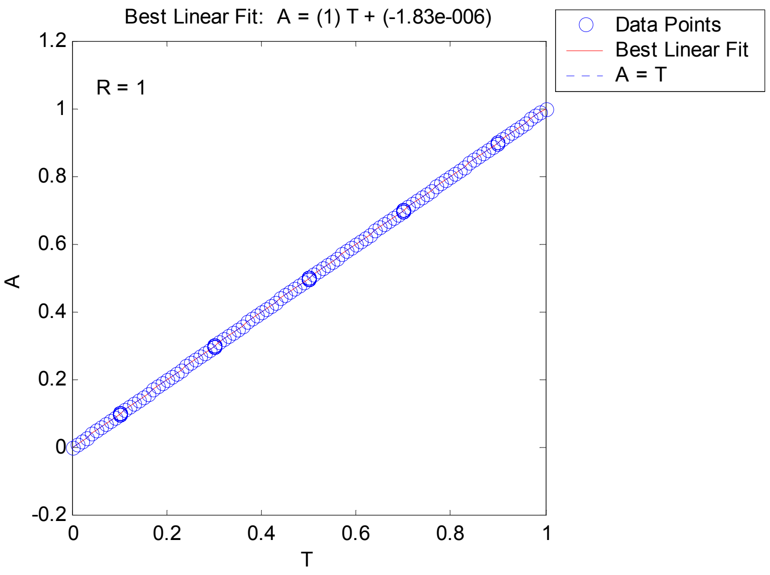

- Regression analysis: **linear fit**
- Correlation coefficient **R = 1**
- Perfect **fit** within **10^{-6}**

Neural Network Performances:
Coffee Canopy Simulation Scene

Coffee-Canopy: LCM input parameters							
Chlorophyll	**Water**	**Lignin**	**Cellulose**	**LAI**	**LAD**	**Sun A**	**Soil R**
37.8 %	6.0e-4	1.2e-3	7.2e-1	0.8	planophile	25 deg	0.3

	Real	**NN**	**Real**	**NN**	**Real**	**NN**	**Real**	**NN**
Leaf **Under-ripe** **Ripe** **Over-ripe**	0.3654 0.1400 0.0589 0.4357	0.3655 0.1398 0.0588 0.4360	0.3603 0.0493 0.0839 0.5065	0.3592 0.0495 0.0840 0.5073	0.2536 0.0721 0.2920 0.3824	0.2533 0.0718 0.2924 0.3824	0.3358 0.0534 0.3567 0.2541	0.3354 0.0533 0.3572 0.2541
Leaf **Under-ripe** **Ripe** **Over-ripe**	0.4983 0.0595 0.0890 0.3532	0.4977 0.0592 0.0893 0.3538	0.2713 0.1614 0.0287 0.5385	0.2711 0.1617 0.0284 0.5387	0.0922 0.4249 0.1662 0.3168	0.0933 0.4246 0.1661 0.3160	0.4516 0.1472 0.1879 0.2134	0.4525 0.1462 0.1882 0.2131
Leaf **Under-ripe** **Ripe** **Over-ripe**	0.4906 0.0712 0.1750 0.2632	0.4904 0.0707 0.1755 0.2634	0.2460 0.3418 0.1122 0.3001	0.2477 0.3409 0.1120 0.2993	0.4433 0.0147 0.2816 0.2604	0.4427 0.0143 0.2823 0.2607	0.2618 0.1663 0.0877 0.4842	0.2623 0.1660 0.0876 0.4841
Leaf **Under-ripe** **Ripe Over-** **ripe**	0.4435 0.0142 0.2219 0.3204	0.4425 0.0140 0.2225 0.3209	0.2280 0.1722 0.3557 0.2440	0.2283 0.1723 0.3558 0.2436	0.0490 0.2861 0.2512 0.4136	0.0494 0.2866 0.2508 0.4132	0.1310 0.2093 0.4551 0.2047	0.1314 0.2093 0.4552 0.2042

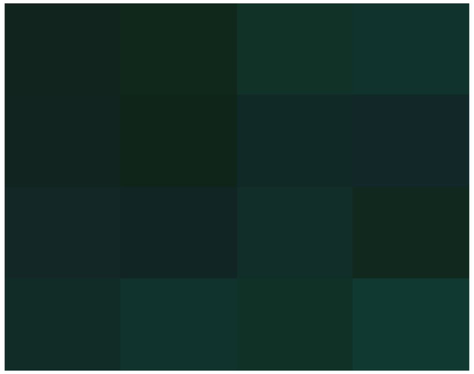

Error Range:

$$10^{-3} \div 10^{-5}$$

Neural Networks for Airborne UAV images

- The NN technique is be applied to UAV airborne images
- Images come from the 2002 Kauai (Hawaii) campaign
- UAV images available at three bands: 580, 660 and 790 nm (visible & infrared)
- Fairly cloud-free, atmosphere corrected collages of images
- DNs-Reflectance transformation performed at NASA Ames
- Parchment data available
- Missing a-priori information
- Multiple NNs required
- Use Domain Projection Technique

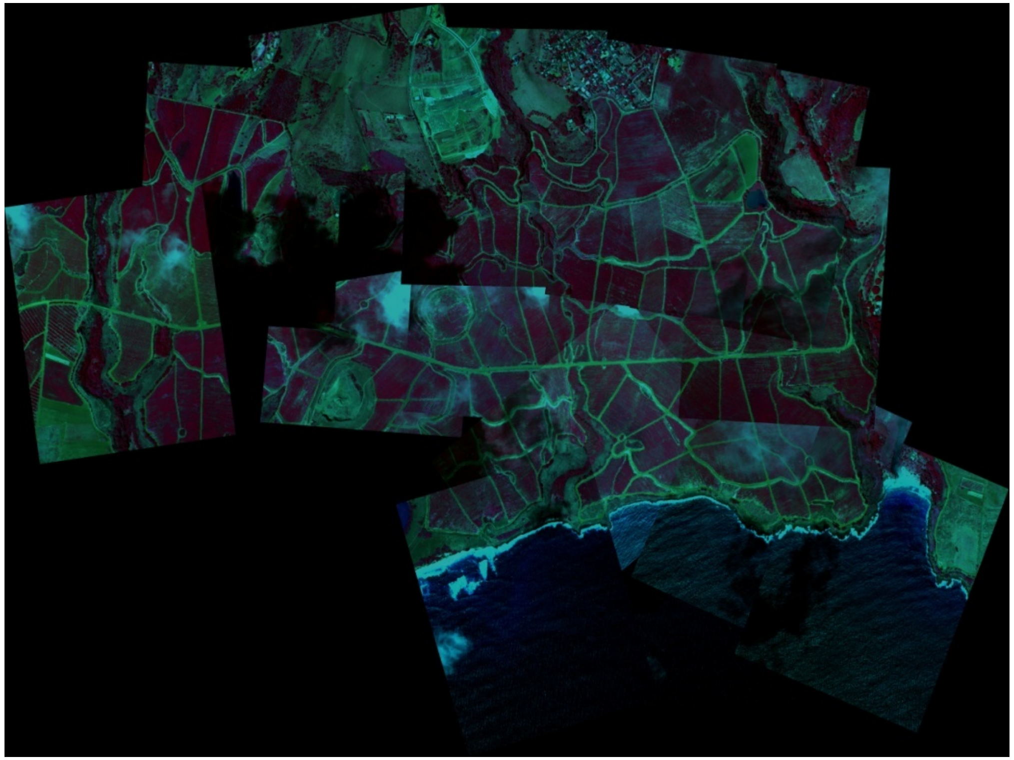

Domain Projection Technique: Overview

- Any NN learns the provided training data set: Extrapolation is unphysical
- Model and measurement errors: Reflectance outside the training set
- Domain Projection Technique (DPT): Project the reflectance back into domain
- Marching toward the central point with three different speeds
- Monitor the network output: Stop when results are physical
- Correction technique required

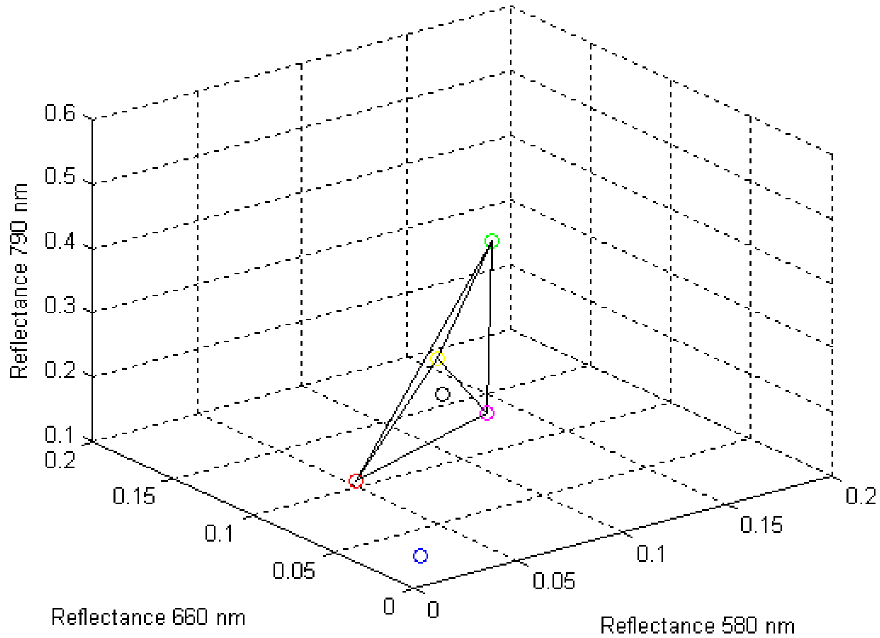

Domain Projection Technique: Application

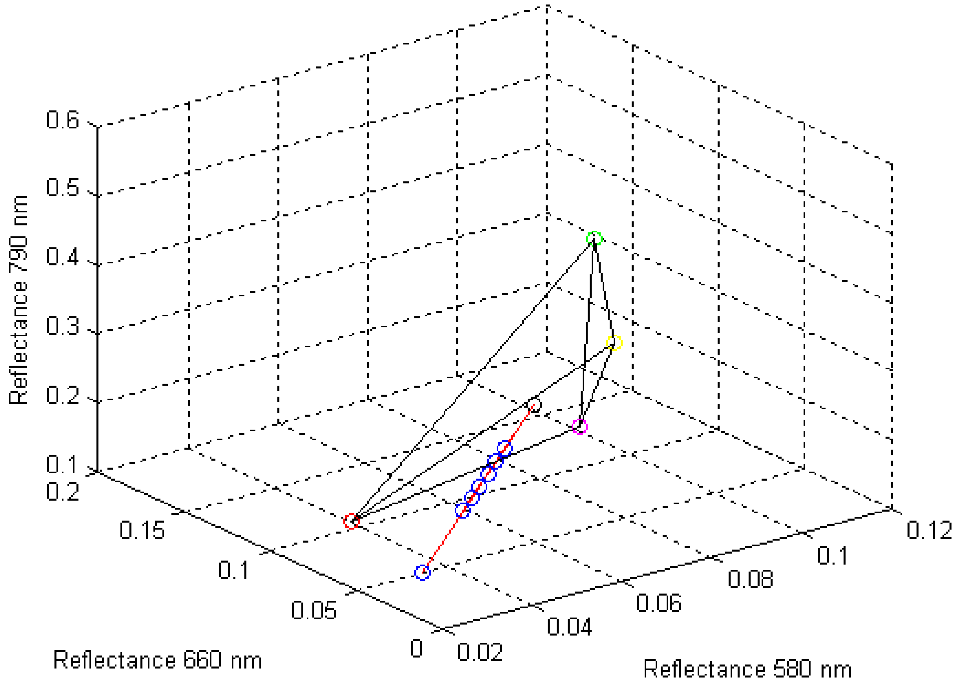

Unphysical

Physical

	Ref 1	Ref 2	Ref 3	Ref 4	Ref 5	Ref 6	Ref 7	Ref 8
Leaf %	**-1.339**	-0.761	-0.305	-0.227	-0.152	-0.082	-0.015	**0.047**
Under-ripe %	**2.165**	1.515	0.973	0.876	0.783	0.693	0.607	**0.524**
Ripe %	**-0.625**	-0.384	-0.146	-0.099	-0.052	-0.006	0.040	**0.086**
Over-ripe %	**0.799**	0.630	0.478	0.450	0.422	0.394	0.367	**0.341**
Speed	**Med**	**Med**	**Low**	**Low**	**Low**	**Low**	**Low**	**Low**

Multiple NNs and DPT Coupled Algorithm

- **Missing a-priori information: 27 neural networks trained**
- **MATLAB image processing and algorithm implementation performed**

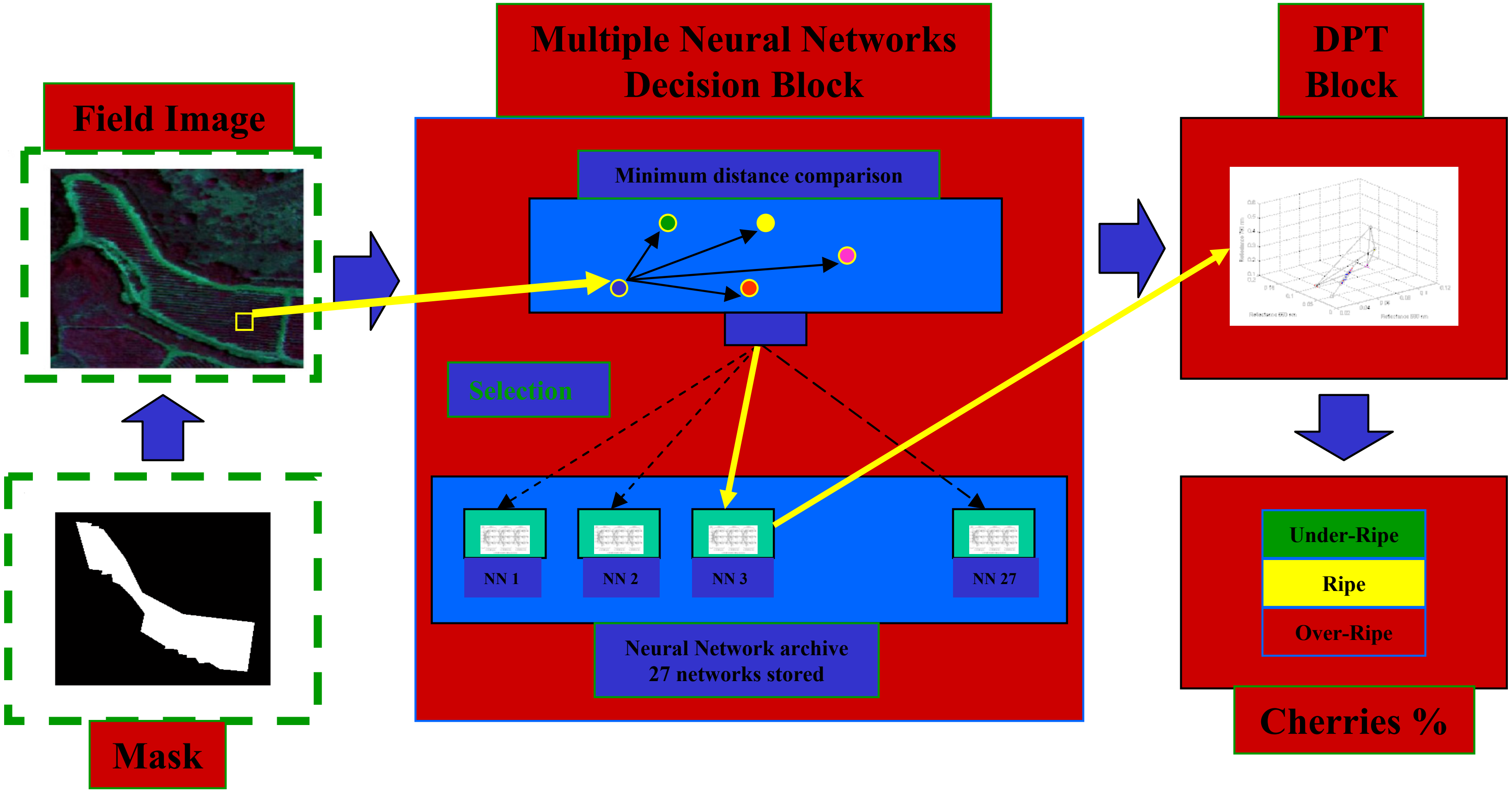

Processing the UAV images: Fields and Blocks

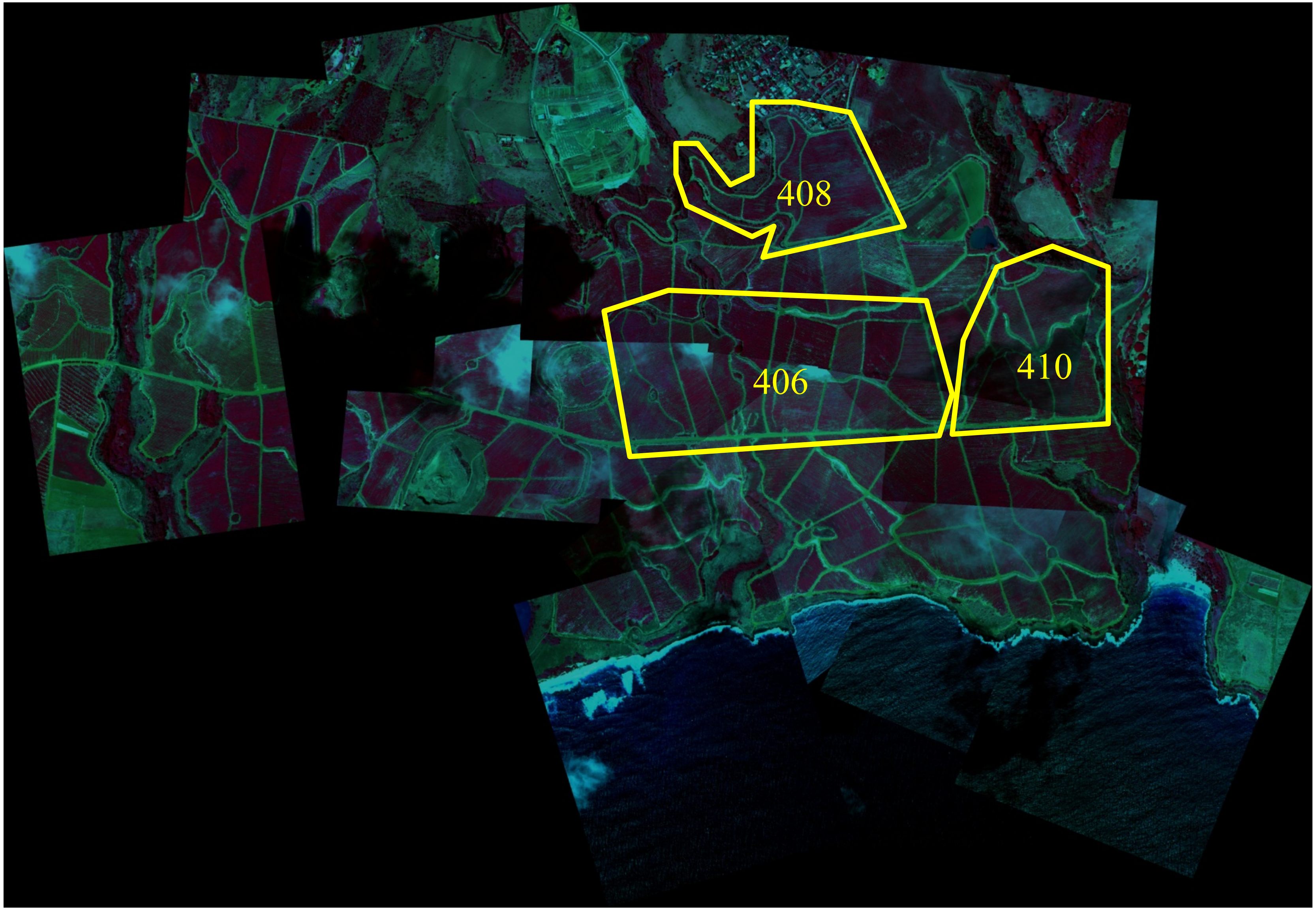

NN prediction vs Parchment data & Branch Count

Field 408				
	Under-ripe %	Ripe % (R)	Over-ripe %(O)	R + O %
Parchment Data	39.45	39.55	21.00	60.55
Neural Network	36.39	25.10	38.49	63.59
Branch Count	x	21.14	47.08	68.22
Error NN %	3.06	14.45	17.49	3.04
Error Branch %	x	18.41	26.08	7.67

Field 406				
	Under-ripe %	Ripe % (R)	Over-ripe %(O)	R + O %
Parchment Data	52.51	17.30	30.19	47.49
Neural Network	49.11	20.97	29.90	50.87
Branch Count	x	34.33	58.53	92.86
Error NN %	3.40	3.67	0.29	3.38
Error Branch %	x	17.03	28.34	45.37

Field 410				
	Under-ripe %	Ripe % (R)	Over-ripe %(O)	R + O %
Parchment Data	71.61	15.14	13.25	28.39
Neural Network	49.58	17.08	33.33	50.41
Branch Count	x	24.07	51.08	75.15
Error NN %	22.03	1.94	20.08	22.02
Error Branch %	x	8.93	37.83	46.76

NN Ripeness Prediction Maps: Field 408 Block 4

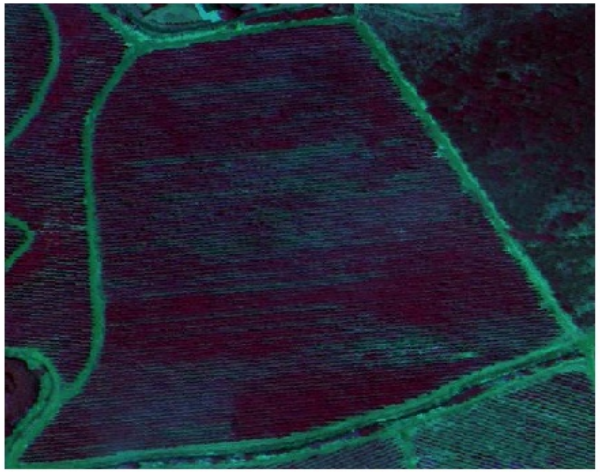

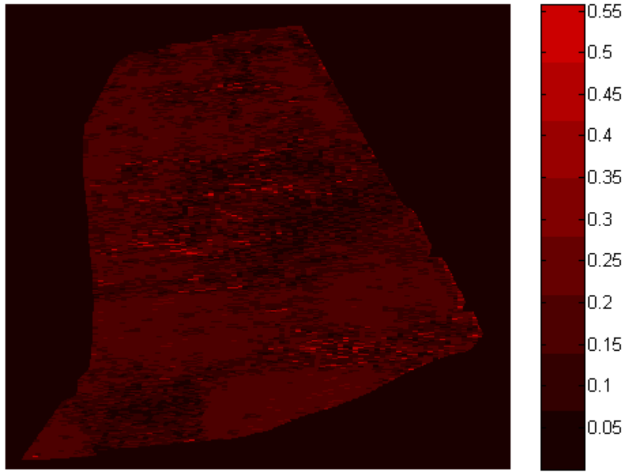

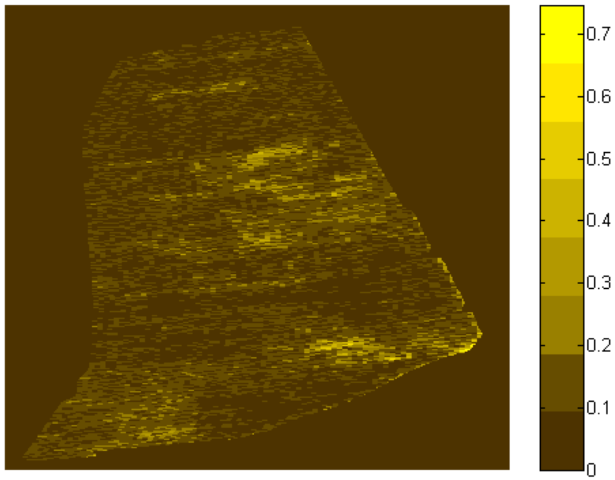

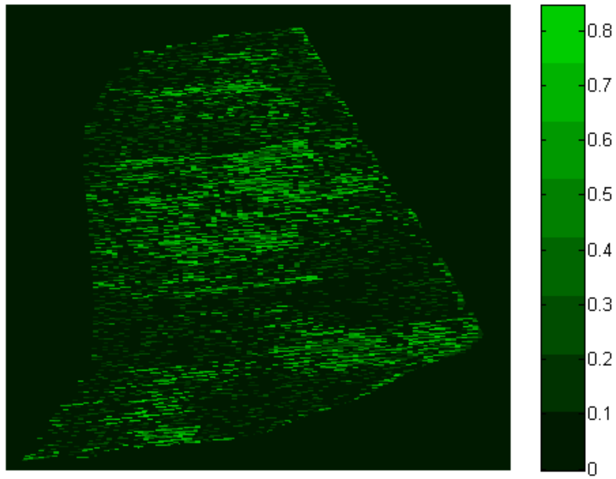

Conclusions

- **NASA Coffee Project:** **Intelligent tool for precision agriculture devised**
- **Modeling radiative regime within canopies: LCM2 for coffee canopies**
- **Neural Network approach: Solution of the inverse problem**
- **Domain Projection Technique developed as remedy to unphysical results**
- **NN Decision Block coupled with DPT form the backbone of the method**
- **Application to UAV images shows the potential of the methodology**